Molecular Therapy
Methods & Clinical Development
Original Article

A Library-Based Screening Strategy for the Identification of DARPins as Ligands for Receptor-Targeted AAV and Lentiviral Vectors

Jessica Hartmann,[1] Robert C. Münch,[1] Ruth-Therese Freiling,[1] Irene C. Schneider,[1] Birgit Dreier,[2] Washington Samukange,[1] Joachim Koch,[3] Markus A. Seeger,[4] Andreas Plückthun,[2] and Christian J. Buchholz[1]

[1]Molecular Biotechnology and Gene Therapy, Paul-Ehrlich-Institut, 63225 Langen, Germany; [2]Department of Biochemistry, University of Zurich, 8057 Zurich, Switzerland; [3]Institute of Medical Microbiology and Hygiene, University of Mainz Medical Center, 55131 Mainz, Germany; [4]Institute of Medical Microbiology, University of Zurich, 8006 Zurich, Switzerland

Delivering genes selectively to the therapeutically relevant cell type is among the prime goals of vector development. Here, we present a high-throughput selection and screening process that identifies designed ankyrin repeat proteins (DARPins) optimally suited for receptor-targeted gene delivery using adeno-associated viral (AAV) and lentiviral (LV) vectors. In particular, the process includes expression, purification, and *in situ* biotinylation of the extracellular domains of target receptors as Fc fusion proteins in mammalian cells and the selection of high-affinity binders by ribosome display from DARPin libraries each covering more than 10^{12} variants. This way, DARPins specific for the glutamate receptor subunit GluA4, the endothelial surface marker CD105, and the natural killer cell marker NKp46 were generated. The identification of DARPins best suited for gene delivery was achieved by screening small-scale vector productions. Both LV and AAV particles displaying the selected DARPins transduced only cells expressing the corresponding target receptor. The data confirm that a straightforward process for the generation of receptor-targeted viral vectors has been established. Moreover, biochemical analysis of a panel of DARPins revealed that their functional cell-surface expression as fusion proteins is more relevant for efficient gene delivery by LV particles than functional binding affinity.

INTRODUCTION

Genetic modification of cells has become one of the most important technologies not only in basic life science but also in gene therapy. From a portfolio of gene delivery vehicles, lentiviral (LV) vectors and vectors derived from adeno-associated virus (AAV) are most often used. Whereas LVs stably integrate their genetic information into the genome of the transduced cells, AAV vectors remain episomal.[1] Therefore, AAVs are better suited for terminally differentiated cells or if short-term gene expression in dividing cells is required, whereas LVs are preferred when stem cells or dividing cells need to be genetically modified.

Regardless which type of gene delivery vehicle is used, the main goal for gene transfer is to deliver genetic information with high efficiency precisely to the therapeutically relevant cell type of interest not only *ex vivo* in cell culture, but also *in vivo* after local or systemic administration. Attempts to tackle this challenge focus on restricting transgene expression either by altering regulatory sequences within the vector genome[2] or by modifying cell entry features through vector surface engineering.[3,4] Vector surface engineering controls the first step in gene transfer, the binding of the vector particle to its cell-surface receptor. Several approaches have been developed to modify the interaction of the vector particles with cell-surface receptors, including designed ankyrin repeat protein (DARPin) adaptors bridging between adenoviruses and target receptors,[5,6] permanent modification of viral capsids, or envelope proteins by incorporation of receptor-binding moieties or evolution-based engineering strategies.[7] A complete re-direction of LV vectors to rare target cell populations with low or even absent off-target activity on non-target cells was achieved by permanent ablation of natural receptor binding and genetic fusion of a targeting ligand that binds the extracellular part of the selected target receptor with high affinity to the vector surface.[8] This engineering concept has been successfully implemented for envelope glycoproteins from Sindbis virus,[9,10] Tupaia virus,[11] measles virus (MV),[12] and recently Nipah virus (NiV)[13] that have the receptor-attachment and membrane-fusion functions separated onto two glycoproteins.

Although fundamentally different in their physical properties, this rational engineering concept is applicable also to non-enveloped AAV particles.[14,15] Whereas single-chain antibodies (scFvs) have been mainly used as targeting ligands for LV vectors, these molecules are not applicable to AAV vectors as genetic fusion, because they are not compatible with the assembly of the AAV particles under reducing conditions in the cell nucleus. DARPins, in contrast, can be used for receptor-targeting of LV, AAV, adenoviral (AdV), and

Received 28 March 2018; accepted 1 July 2018;
https://doi.org/10.1016/j.omtm.2018.07.001.

Correspondence: Christian J. Buchholz, Molecular Biotechnology and Gene Therapy, Paul-Ehrlich-Institut, Paul-Ehrlich-Str. 51-59, 63225 Langen, Germany.
E-mail: christian.buchholz@pei.de

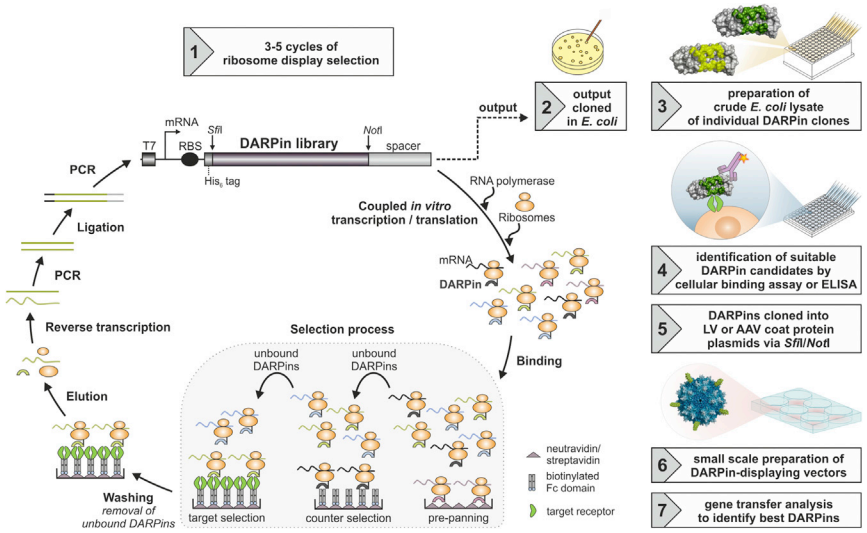

Figure 1. Workflow for the Selection of DARPins for Receptor-Targeted LVs and AAVs

DARPin selection by ribosome display is shown in steps 1 and 2. All substeps of the ribosome display cycle are performed cell-free *in vitro*. Each cycle begins with the transcription and translation of a DARPin-encoding DNA library, flanked by a T7 promoter (T7), a ribosome binding site (RBS), and a spacer sequence. Ternary complexes of ribosome, the DARPin-encoding mRNA, and the translated polypeptide (shown in identical color) are formed and allowed to bind to the target protein during the selection process. The selection process encompasses three steps: pre-panning, counter-, and target selection. Pre-panning and counter-selection results in the elimination of the black and brown DARPins binding to the Fc domain or streptavidin used for immobilization of the target receptor. The green DARPin, in contrast, binds the target receptor and is carried forward to the next selection cycle. After the selection process, unbound complexes are washed away before elution, and reverse transcription of the mRNA is carried out. The cDNA fragments are PCR amplified and ligated to the upstream and downstream flanking sequences. The PCR-amplified ligation product is used as template library for the next ribosome display cycle or cloned into an expression vector for analysis of single clones on the protein level. After ribosome display, individual DARPin molecules are expressed as crude *E. coli* lysates (step 3), tested for their receptor binding ability (step 4), and subcloned into the corresponding viral vector plasmids (step 5) before small-scale generation of DARPin-displaying LV or AAV particles (step 6), which are finally analyzed for cell-type-specific gene transfer (step 7). Exemplarily an AAV vector is shown displaying five molecules of an individual DARPin clone on its surface, but the same procedure is applied for LV particles. Step 1 of the figure is adapted from Dreier and Plückthun.[53]

oncolytic MV vectors.[8,16,17] Notably, this way such different vector types as LV and AAV can be generated in a way to use an identical binding domain for cell entry.[14,15,18]

Adapted from naturally occurring ankyrin repeat proteins, DARPins are based on small (14–17 kDa), highly stable, α-helical scaffolds with a very low tendency to aggregate.[19] By diversifying seven residues within each repeat domain (33 amino acids) and by combining 2–3 repeats flanked by short N- and C-terminal capping modules, combinatorial DARPin libraries covering more than 10^{12} variants have been generated.[20,21] The first combinatorial DARPin library was based on consensus design utilizing a database with a large number of unbiased ankyrin repeat protein sequences.[20] Subsequently, this design was improved by introducing point mutations into the C-terminal capping module to stabilize the DARPins, while the remaining framework remained unchanged.[22] The design by Seeger et al.[21] encompasses one additional diversified position in each repeat domain and three diversified positions in the C-terminal capping module and changes in the overall framework ending up in a DARPin library with reduced hydrophobicity and an extended randomized surface. Using ribosome display, DARPins binding to basically any protein of interest with affinities in the range of antibodies can be obtained.[23] Ribosome display is an *in vitro* evolution process in which the DARPin (phenotype) is physically coupled to its genetic information (genotype) within the ribosome.[24] This is achieved by forming stable ternary complexes of the encoding mRNA, the ribosome, and the nascent DARPin polypeptide chain. Notably, libraries covering very large repertoires of DARPin variants can be selected by this approach, since the whole process operates cell free. Accordingly, the selection process usually results in a diverse pool of target-binding DARPins from which the best candidates have to be identified individually.[23]

We report here proof of principle for a selection process that integrates the screening in context of vector particles and thus identifies DARPins suitable for receptor-targeted AAV and LV particles. Chosen target receptors included the glutamate receptor subunit GluA4, a marker for a subpopulation of inhibitory interneurons being highly relevant for various neurological disorders such as epilepsy,[25] the activating natural killer (NK) cell receptor NKp46,[26] a ubiquitous NK cell marker, and endoglin (CD105), a marker for tumor-related angiogenesis.[27] These served as target for the selection of various DARPin libraries, including two newly generated libraries, each covering more than 10^{12} variants optimized for straightforward subcloning into viral vector packaging plasmids. Of the pools of DARPins selected for each target receptor, those best suited for cell-type-specific gene transfer with LV or AAV were identified. Biochemical analysis of the DARPins revealed correlations among functional target receptor binding affinity, cell-surface expression levels when fused to an LV envelope protein, and gene delivery. Taken together, the data provide proof of concept for a high-throughput approach of selecting and identifying targeting ligands for viral vectors and provide some insights into distinct requirements of DARPins for LV and AAV re-targeting.

RESULTS

The process for the selection of DARPins compatible with receptor targeting of AAVs and LVs is shown in Figure 1. For straightforward purification, the extracellular part of the target receptor is

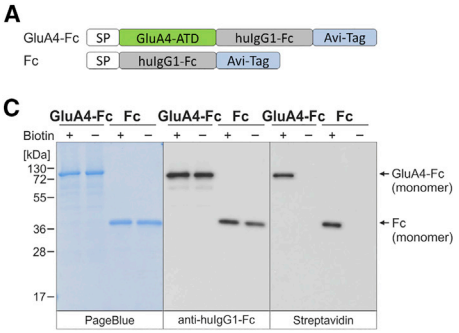

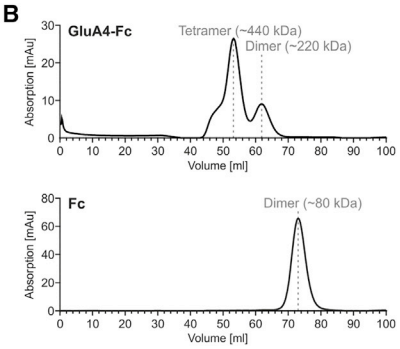

Figure 2. Expression and Purification of Recombinant Target Proteins for Ribosome Display

(A) Schematic drawing of GluA4-Fc and Fc, two recombinant proteins used as targets for ribosome display. The GluA4-Fc construct consists of the amino-terminal domain (ATD) of the glutamate receptor subunit 4 (GluA4) fused N-terminally to the Ig kappa chain signal peptide (SP) and C-terminally to the constant region of human IgG1 (huIgG1-Fc) for detection and purification and an Avi tag for biotinylation. As control in selections, only huIgG1-Fc with Avi tag were expressed (directly fused to the signal peptide). (B) Chromatograms of size exclusion chromatography (SEC) of proteins expressed in and purified from the cell culture supernatant of HEK293T cells via protein A. The calculated molecular weight of the corresponding peaks is indicated. (C) Reducing SDS-PAGE and western blot analysis of SEC-purified GluA4-Fc and Fc proteins produced in the absence (−) or presence of biotin (+) added to the culture. 2 μg and 20 ng of purified proteins were loaded onto 10% SDS gels, respectively. Purified proteins were visualized by PageBlue protein staining solution and detected by a huIgG1-Fc-specific antibody. Biotinylated proteins were detected using streptavidin-HRP.

expressed in HEK293T cells fused to the fragment crystallizable (Fc) domain of immunoglobulins. Biotinylation of the expressed target receptor is performed during production in HEK293T cells.[28] Importantly, the used DARPin libraries contain compatible restriction sites to allow easy subcloning into the viral vector coat protein plasmids. After initial ribosome-display-based binder selection, target receptor binding is verified by ELISA or flow cytometry followed by downstream screening steps involving small-scale high-throughput compatible production of vector particles in multi-well plates and transduction of target-receptor positive and negative cell lines. Notably, during ribosome display, DARPins binding to the Fc part of the recombinant target receptor or to biotin are removed through pre-panning and counter-selection steps (Figure 1).

Construction of DARPin Libraries Optimized for Viral Vector Display

To enable a fast and efficient selection process and subsequent incorporation into viral vectors, we generated two DARPin libraries that were optimized for translation in *E. coli* and harbor unique restriction sites compatible with our vector-targeting platform. The viral vector (VV) compatible DARPin libraries VV-N2C and VV-N3C were assembled from *de novo* synthesized DNA fragments encoding the diversified ankyrin repeats as well as the N- and C-terminal capping modules based on previously published DARPin library sequences.[23] Upon subsequent ligation and PCR amplification, we generated DARPin libraries consisting of two (VV-N2C) and three (VV-N3C) diversified repeats in-between the constant N- and C-capping modules, respectively (Figure S1). Each DARPin library covered at least 10^{12} DARPin molecules, after ligation of the flanking regions needed for ribosome display to the assembled library as estimated from the amount of ligated DNA before PCR amplification (Table S1). Sequence analysis of 100 clones of each library revealed a constant framework with incidental point mutations but no frameshifts, harboring seven diversified amino acid positions within each ankyrin repeat for 81% (VV-N2C) and 60% (VV-N3C) of the clones (Figure S2).

Selection of GluA4-Specific DARPins

GluA4 is composed of an extracellular amino-terminal domain (ATD), an extracellular ligand-binding domain, a transmembrane domain, and an intracellular carboxyl-terminal domain.[29] For the DARPin selection process, the ATD of murine GluA4 was fused to the constant region of human immunoglobulin G1 (huIgG1-Fc) and an Avi tag, resulting in GluA4-Fc (Figure 2A). As control, the huIgG1-Fc fused to the Avi tag (Fc) was generated (Figure 2A). The proteins were produced in a biotinylated and unbiotinylated form by expression in HEK293T cells transfected with a plasmid encoding the *E. coli*-derived biotin ligase BirA, an enzyme enabling specific biotinylation of the Avi tag in the presence of biotin and ATP.[28] GluA4-Fc and Fc were purified to homogeneity from the culture medium by protein A affinity purification and subsequent preparative size exclusion chromatography resulting in approximately 1 mg of pure protein from 10^8 cells. The GluA4-Fc protein consisted mainly of tetramers, and, to a lesser extent, of dimers and larger oligomers (Figure 2B). This reflects the tetrameric structure of glutamate receptors build from dimers.[30] The Fc protein solely formed disulfide-linked homodimers (Figure 2B). All of the oligomers disassembled to monomers under denaturing and reducing conditions (Figure 2C). Only the proteins produced by BirA-expressing HEK293T cells were detectable by streptavidin (Figure 2C). Roughly 76% of GluA4-Fc protein and 63% of the Fc protein produced in the presence of BirA ligase were biotinylated as determined by ELISA using a biotinylated reference standard.

GluA4-Fc was then used to select DARPins specific for GluA4 from the newly generated VV-N2C and VV-N3C libraries as well as from the N3C DARPin library with reduced hydrophobicity (S-N3C).[21] Specific DARPins were isolated from these libraries by performing five ribosome display selection rounds against the tetrameric GluA4-Fc molecule, including pre-panning steps against neutravidin or streptavidin as well as counter-selection steps against Fc and biotin to prevent the selection of unspecific or Fc-specific binders. For further screening, individual DARPins from the selected pools were expressed in *E. coli* (Figure S3A) and then

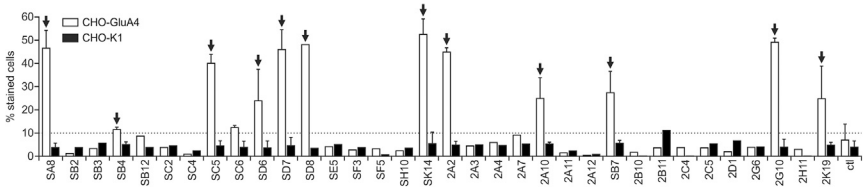

Figure 3. Identification of DARPin Clones Binding to Cell-Surface-Exposed GluA4

Crude *E. coli* extracts of randomly picked clones obtained as output of the ribosome display selection procedure were analyzed for binding to GluA4-positive and -negative CHO cells (CHO-GluA4 and CHO-K1) via flow cytometry. The percentage of cells bound by the DARPin clone is shown. *E. coli* extracts without DARPin were used as control (ctl). Arrows indicate selected DARPins used for further analysis. See also Figure S3.

assessed for binding to GluA4-Fc and to Chinese hamster ovary (CHO)-GluA4 cells directly from crude bacterial lysates. This way, we identified 12 candidates that bound efficiently to GluA4-Fc and CHO-GluA4 cells, but not to GluA4-negative CHO cells or recombinant Fc (Figures 3 and S3B).

GluA4-DARPins Mediate Gene Transfer of LV and AAV Vectors

In order to evaluate the capacity of the selected DARPins to redirect the tropism of LV and AAV vectors to GluA4, they were fused to the H protein of MV and the VP2 protein of AAV-2 for pseudotyping of LV and AAV vectors, respectively. The targeting potential of the corresponding LV and AAV vector particles was determined by transduction of GluA4-positive and negative CHO cells (CHO-GluA4 and CHO-K1). As negative control, the epithelial cell adhesion molecule (EpCam)-specific DARPin Ec1[31] was used for both LV and AAV vectors,[14] while as positive control the single-chain Fv (scFv) recognizing GluA4 and GluA2 (Fab7) was applied to LV vectors only.[12] Unmodified AAV-2 particles or LV particles pseudotyped with VSV-G were used as controls. For AAV particles, six out of the 12 DARPin candidates (SC5, SD7, SD8, 2A2, 2K19, SK14) generated more than 10% transduced CHO-GluA4 cells. This rate was clearly above the 5% background transduction rate observed with the control DARPin or on CHO-K1 cells with all DARPins tested (Figure 4A). Notably, none of the selected DARPin-mediated transduction of CHO-K1 cells above the background level. However, only DARPins SD8, SK14, and 2K19 mediated a significantly enhanced transduction of target compared to non-target cells. Among these, 2K19 mediated the by far highest transduction rate with AAV (Figure 4A).

For LV particles, background transduction was in general much lower than with the AAV vectors (Figure 4). Six DARPin candidates (SB4, SK14, 2A2, 2B7, 2G10, and 2K19) mediated significantly enhanced and selective transduction of the CHO-GluA4 cells compared to CHO-K1 (Figure 4B). Notably, at least two DARPins (SB4 and SK14) were more efficient in mediating gene transfer than the scFv Fab7. Overall, the most effective DARPins for re-targeting of LV particles were SB4, SK14, and 2K19, whereas for AAV particles, SD8, SK14, and 2K19 were the best candidates. Interestingly, only two DARPins (2K19 and SK14) mediated efficient gene transfer for both LV and AAV particles.

To demonstrate that cell entry was indeed mediated by the DARPins, vector stocks were pre-incubated with recombinant GluA4-Fc or Fc protein prior to transduction of target and non-target cells. Pre-incubation with GluA4-Fc resulted in complete abrogation of specific gene transfer on CHO-GluA4 cells for both AAVs and LVs (Figures 4C,4D, and S4). In contrast, pre-incubation with Fc protein had no influence on the transduction efficiency, which was then comparable to that observed with untreated vector stocks.

GluA4-DARPin-Displaying Vectors Are Highly Target Specific

After identification of the most effective DARPins for LV and AAV retargeting, we next assessed their receptor specificity by transducing cell lines expressing the closely related family members GluA1–3 or the non-related kainate receptor GluR6 (Figures 5 and S5). None of the vector stocks displaying the selected DARPins mediated specific gene transfer of cells expressing GluA1–3 or GluR6, while efficient gene transfer of CHO-GluA4 was demonstrated (Figures 5 and S5). In contrast, the LV vector displaying the Fab7-scFv transduced CHO-GluA4 and CHO-GluA2 cells (Figures 5B and S5C). These data demonstrate that the selected DARPins can readily discriminate between GluA4 and its closely related family members.

Selected DARPins Bind to GluA4 with High Affinity

Next, we characterized the selected DARPins at the molecular level. Their sequences are aligned in Figure S6. Whereas 2K19 as well as 2A2, 2A10, 2B7, and 2G10 were derived from the VV-N2C library, SK14 as well as SA8, SB4, SC5, SD6, SD7, and SD8 were derived from the S-N3C DARPin library. Interestingly, DARPin 2K19 is an N1C DARPin comprised of only one single repeat domain besides the capping domains. Next, two DARPins (2K19 and SK14) with the most favorable targeting properties for both LV and AAV vectors as well as SD8, which only mediated gene transfer for AAV, were expressed in *E. coli* and purified to homogeneity for further investigations (Figures 6A and S7). In the next step, the apparent binding affinity to GluA4 was estimated by ELISA. The selected DARPins bound to GluA4 with high affinity in the lower nanomolar range (K_D < 5 nM). The receptor specificity was determined on cell lines expressing GluA4, GluA1, GluA2, or GluA3. All three selected DARPins bound to CHO-GluA4 cells and showed no cross-reactivity to GluA1 and GluA3 or the parental CHO-K1 cell line (Figure 6B). Interestingly, DARPins SD8 and 2K19 explicitly recognized GluA4, whereas SK14 bound CHO-GluA2 cells as well, even though to a lower, not significantly enhanced extent (Figure 6B). Although SK14 was able to bind to GluA2, it did not mediate gene transfer via this receptor when displayed on LV or AAV vectors (Figure 5).

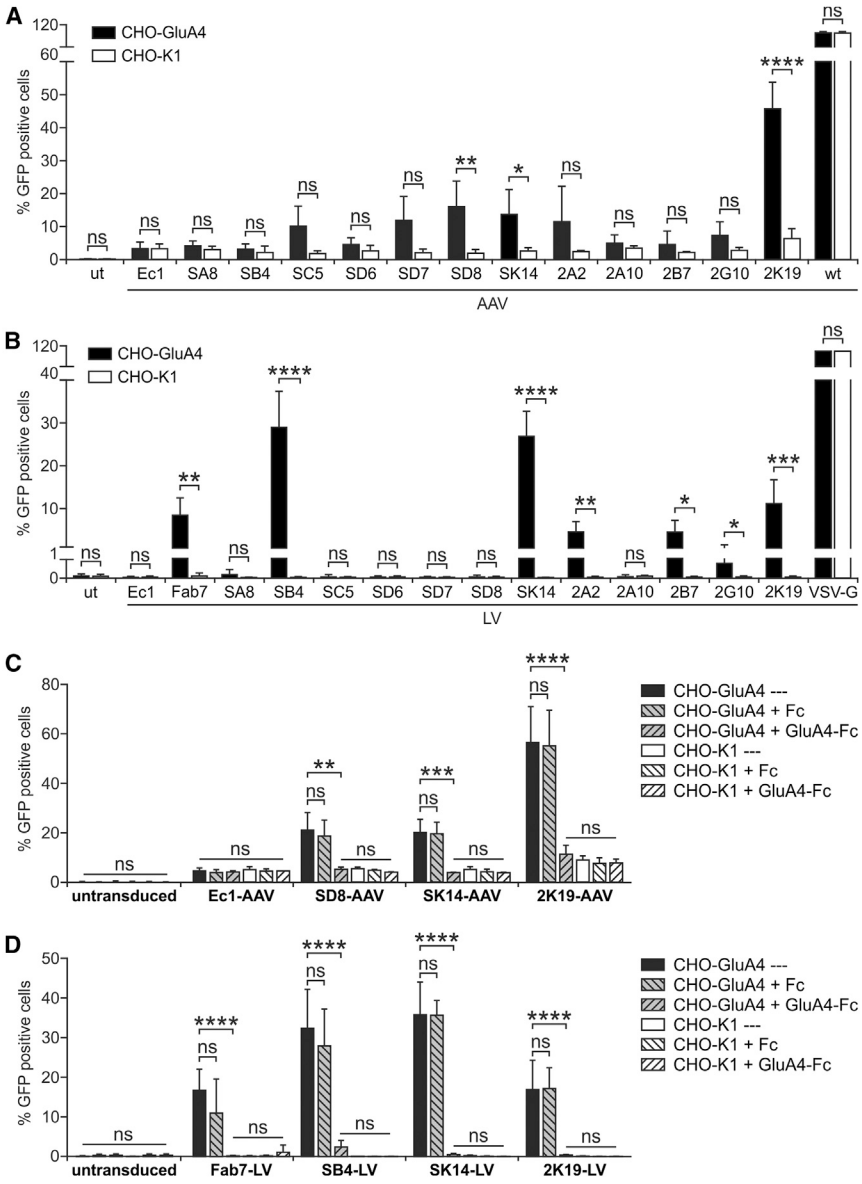

Figure 4. Identification of GluA4-Specific DARPins Mediating Transduction by AAV and LV Vector Particles

The identified GluA4-binding DARPins were cloned into the expression plasmids pDARPin-VP2 as well as pCG-HΔ18-DARPin, which were used to produce GluA4-targeted AAV and LV particles in small-scale multi-well plates in a total volume of 750 μL, respectively. (A and B) CHO-GluA4 and CHO-K1 cells were incubated with 50 μL AAV (A) or 50 μL LV (B) particles encoding GFP. Cells were analyzed 72 hr after transduction by flow cytometry. Untransduced (ut) cells and AAV particles displaying the EpCAM-specific DARPin Ec1 were used as negative control. Unmodified AAV particles (AAVwt) were used as positive control. For LVs, particles displaying the scFv Fab7 or pseudotyped with VSV-G were used as positive control. Each transduction experiment was performed at least three times with individually produced vector stocks. For all experiments, the mean and SD are shown. ****$p \leq 0.0001$; ***$p \leq 0.001$; **$p \leq 0.01$; *$p \leq 0.05$; ns, not significant by unpaired t test comparing target versus non-target cells per vector sample. (C and D) For the best performing AAV (C) and LV (D) particles a competition assay was performed by incubation of the vector particles with recombinant GluA4-Fc and Fc proteins, respectively, or buffer as control prior to transduction of CHO-K1 or CHO-GluA4 cells. In all experiments, the cells were analyzed for GFP expression 72 hr post-transduction by flow cytometry. Untransduced cells and AAV particles displaying the EpCAM-specific DARPin Ec1 were used as negative controls. Each transduction experiment was performed at least three times with individually produced vector particles, showing mean values and SDs. ****$p \leq 0.0001$; ***$p \leq 0.001$; **$p \leq 0.01$; *$p \leq 0.05$; ns, not significant by one-way ANOVA comparing each condition with each other per vector sample (Tukey's multiple comparisons test). See also Figure S4.

Binding and Surface-Expression Properties Define the Suitability of a DARPin as a Targeting Ligand

Since not all GluA4-binding DARPins mediated gene transfer by LV and/or AAV, we next evaluated biochemical parameters of the DARPin fusion constructs and vectors. On vector particles, DARPins are displayed as fusion protein, in conjunction with the MV H protein for LV, and the VP2 protein for AAV vectors. For incorporation into LV particles, the DARPin-H fusion protein has to be efficiently expressed at the cell surface. To assess the surface expression of the DARPin-H constructs, HEK293T cells were transfected with the corresponding expression plasmids and analyzed for protein presentation by flow cytometry utilizing the His tag present on the MV H fusion protein (Figures 7A and S8). Out of 10 tested DARPin-H constructs, DARPins SK14, SB4, 2K19, 2B7, SD8, SD7, and SC5 showed high surface-expression rates within a similar range (mean fluorescence intensity [MFI] of 815 to 1,417). Two DARPins (SD6 and 2G10) resulted in substantially weaker surface expression (MFI of 154 to 213), in the range of that of the scFv Fab7 fused to the H protein, and only one DARPin (2A10) was not detectable at all (Figures 7A and S9C). Notably, analysis of the particle composition by western blot revealed a clear positive correlation between surface expression and incorporation of the DARPin-H proteins into LV vector particles (Figure S9A).

Next, we evaluated the ability of the corresponding LV vectors to transduce cells independently of binding to the GluA4 receptor. For this purpose, we made use of a His tag C-terminally fused to the DARPin and CHO cells expressing a membrane-bound form of the anti-His scFv 3D5[32] (CHO-αHis cells). Transduction of CHO-αHis cells with DARPin-LV particles demonstrated efficient to moderate gene transfer rates for DARPins with a high surface expression (Figures 7B and S9). DARPins that exhibited weak or no detectable

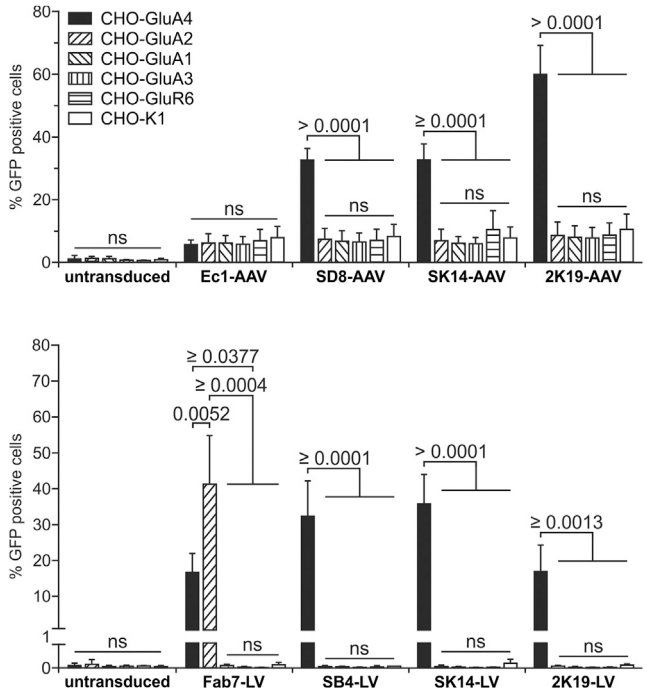

Figure 5. Recognition of Glutamate Receptor Family Members by GluA4-Targeted Vector Particles

To determine the selectivity of the GluA4-targeted vector particles, CHO-K1 cells expressing GluA1-4 or GluR6 as well as the parental cell line were incubated with the indicated AAV (top panel) and LV (bottom panel) particles, respectively. In all experiments, the cells were analyzed for GFP expression 72 hr post-transduction by flow cytometry. Untransduced cells, AAV particles displaying the EpCAM-specific DARPin Ec1 (top panel), or LV particles displaying the GluA2- and GluA4-specific scFv Fab7 (bottom panel) were used as control. Each transduction experiment was performed at least three times with individually produced vector particles, showing mean values, SDs, and p values. ns, not significant; p values by one-way ANOVA comparing each condition with each other per vector sample (Tukey's multiple comparisons test). See also Figure S5.

surface expression as H fusion protein mediated no or very few transduction events. These results reveal a correlation between the amount of incorporated DARPin-H protein and the cell fusion activity of the LV particles on CHO-αHis cells. When directly comparing the gene-transfer rates on CHO-GluA4 and CHO-αHis cells, we can distinguish three groups of DARPins. DARPins SD8, SD7, and SC5 mediated high to moderate gene transfer on CHO-αHis cells but did not, or only inefficiently, transduce CHO-GluA4 cells. DARPins SK14, SB4, and 2K19 efficiently transduced both CHO-αHis and CHO-GluA4 cells, while 2A10, SG10, and SD6 were basically inactive on both cell types.

To assess whether the binding properties of the selected DARPins to GluA4 were altered by fusion to the MV H protein, we assessed binding of the DARPin-H proteins presented on HEK293T cells to varying GluA4-Fc concentrations in a flow-cytometry-based assay. For all DARPins except 2A10, which showed no surface expression, binding curves with the typical sigmoidal shape were obtained (Figures 7C and S8). From these curves, the apparent functional binding affinity, commonly referred to as avidity, was calculated from the GluA4-Fc concentrations required for half-maximal binding. For four DARPins (SD8, SK14, 2K19, 2B7) and the scFv Fab7, these were in the single-digit nanomolar range (apparent K_D = 1.6–3.7 nM) (Figure 7C). DARPins 2B7 and SB4 were slightly less affine (apparent K_D = 8.4 nM and 19 nM). Binding of DARPins SD6, SD7, 2G10, and SC5 was too close to the detection limit to calculate a meaningful value. The maximal MFI obtained in this assay was taken as a measure for the functional binding capacity of cell-surface-displayed DARPins to GluA4. Four DARPins (SB4, SK14, 2B7, and 2K19) showed a relatively high binding capacity, whereas presentation of DARPins SD8, SD6, SD7, 2G10, SC5, or the scFv Fab7 resulted in a 3.5- to 12-fold lower binding capacity (Figure 7C).

To analyze which parameters influence the ability of the selected DARPins to mediate transduction, the apparent surface-binding avidity and the functional binding capacity were correlated with the amount of DARPins presented on the cell surface, respectively. All four DARPins that mediated efficient gene transfer by LVs cluster in this diagram and show high surface expression and binding capacity of GluA4 as MV H fusion protein (Figure 7D). In contrast, DARPins with similar high surface expression but lower GluA4 binding capacity led only to efficient transduction of CHO-αHis but not of CHO-GluA4 cells (Figure 7). This suggests that high surface expression and functional binding capacity are critical for LV vectors, while strong binding avidity can be beneficial but is not essential. While these data are obviously more relevant for LVs, it is interesting to note that the DARPins mediating AAV transduction rather cluster in the diagram correlating binding avidity with surface expression. Those DARPins with calculated apparent binding avidity values of <5 nM mediated transduction by AAV, while the less-affine DARPins 2B7 and SB4 did not (Figures 4 and 7D).

Having the successful selection of GluA4-specific DARPins compatible with receptor targeting of AAVs and LVs demonstrated, we next applied the DARPin selection process for murine CD105, a marker of endothelial cells, and human NKp46, a receptor on NK cells. For CD105, the selections were performed using N2C and N3C DARPin libraries described by Binz et al.,[20] here termed B-N2C and B-N3C. In total, 21 binders were identified from the subsequent cellular binding assay and were screened for their ability to mediate gene transfer (Figures 8A–8C). Eight DARPins, with 2B33 and 3B72 being most efficient, mediated AAV gene transfer substantially above background into CHO cells overexpressing CD105 (CHO-mCD105) (Figures 8B–8C). For NKp46, selections were performed using the VV-N3C library as well as with the S-N3C DARPin library. Promising candidates identified by cellular binding assays were assessed for their surface presentation and binding to recombinant NKp46 upon display on the MV H protein (Figures 8D and 8E). Eight out of 11 tested DARPin-H proteins showed a high surface expression, from which six candidates showed NKp46 binding more than 2-fold over background (Figure 8E). Five out of five tested DARPins displaying LVs mediated gene transfer into HT1080 cells overexpressing NKp46

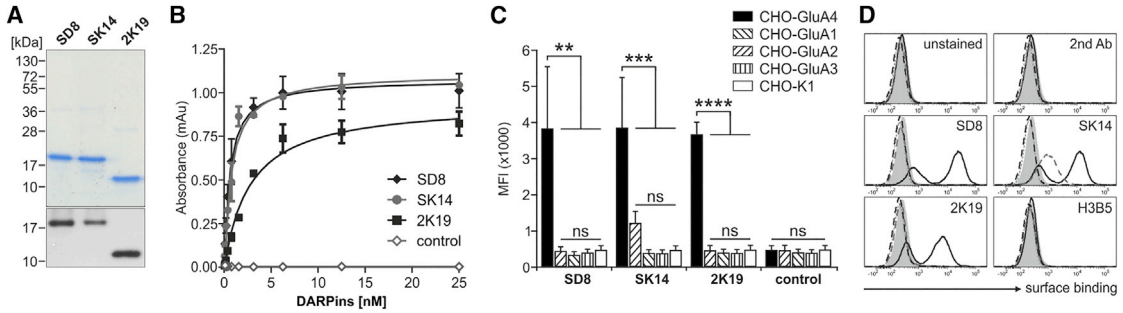

Figure 6. The Identified GluA4-DARPins Bind GluA4 with High Apparent Affinity

(A) Reducing SDS-PAGE and western blot analysis of His-tagged DARPins purified from *E. coli*. 2 μg and 500 ng protein were loaded onto a 15% SDS gel, respectively. Purified proteins were visualized by PageBlue protein staining solution (top) and detected by an anti-His-tag specific antibody (bottom). (B) Binding of graded amounts of DARPin SD8 (gray circles), SK14 (black diamonds), 2K19 (black squares), and the unrelated DARPin H3B5 (open diamonds) to recombinant GluA4-Fc determined by ELISA. (C) Binding of purified DARPins to CHO-K1 cells expressing GluA1-4 or the parental cell line analyzed by flow cytometry. The unrelated DARPin H3B5 was used as control. Mean fluorescent intensity values of three independent experiments represented as bar diagram are shown with mean values and SDs. ****$p \leq 0.0001$; ***$p \leq 0.001$; **$p \leq 0.01$; ns, not significant by one-way ANOVA comparing each condition with each other per DARPin (Tukey's multiple comparisons test). (D) Representative flow cytometry histograms of (C). CHO-GluA1 (gray dotted line), CHO-GluA2 (gray dashed line), CHO-GluA3 (black dashed line), CHO-GluA4 (black solid line), and CHO-K1 (filled curves) cells were either incubated with indicated DARPins or as controls with secondary antibody (2nd Ab) or buffer only (unstained).

(HT1080-NKp46) over background (Figure 8F). Four DARPins (3F9, 3A8, 3E7, and 3C9) mediated transduction efficiencies above 65%. Exactly these DARPins demonstrated high surface expression and receptor binding (Figure 8E).

DISCUSSION

Cell-type-specific delivery of viral vectors has become an important tool not only in basic research but also in gene therapy with first clinical applications.[33] Ablation of natural receptor binding sites and simultaneous genetic fusion of a receptor-specific targeting ligand to the vector surface was demonstrated to be a highly efficient and flexible method to re-direct vectors.[8] DARPins offer several advantages as targeting ligands over antibody scaffolds, because they can be selected for almost any target protein of choice and exhibit favorable properties like high stability, no cysteine bridges, low immunogenicity, and low aggregation tendency.[17]

To work properly as targeting ligand for AAV or LV vector particles, DARPins have to fulfill various requirements. These include (1) binding to the target receptor with high selectivity, (2) efficient expression in mammalian cells as fusion protein with a paramyxoviral attachment protein or the AAV capsid protein, (3) incorporation into the vector particles, and (4) mediating cell entry of the vector particle followed by gene delivery. To select DARPins recognizing target receptors as displayed in their native form on the cell surface, we expressed extracellular parts of the interneuron marker GluA4, the endothelial marker CD105 or the NK cell marker NKp46 as secreted Fc-fusion proteins in mammalian cells. Fc tagging usually results in dimerization but can also be compatible with tetramer formation. Indeed, production of the Fc fusion protein with the ATD of GluA4 yielded dimers and tetramers which is in line with glutamate receptors being composed of four subunits, building dimers of dimers and the ATD being responsible for dimer formation.[29] However, inclusion of a huge protein tag like the huFc part or antibodies to capture the target protein during ribosome display bears the risk of off-target binder selection. To minimize selection of off-target binders, we included several pre-panning and counter-selection steps during the selection process. This strategy efficiently prevented selection of huFc tag-specific DARPins while ensuring enrichment of target-specific binders. In addition, no capture antibody was used. Instead, coupling was ensured by binding of biotinylated target protein to neutravidin or streptavidin.

While the target proteins for ribosome display can be biotinylated *in vitro* or *in vivo*, we adapted here the method of metabolic biotinylation in mammalian cells.[28,34] In this case, protein biotinylation is performed simultaneously to its production within mammalian cells, circumventing additional manipulation of the protein after purification. We used an endoplasmic reticulum (ER)-associated and a secreted form of the *E. coli* derived BirA ligase during production, to allow biotinylation of secreted proteins during intracellular trafficking and within the cell culture supernatant. The successful selection of GluA4- and NKp46-specific DARPins proves that this approach is efficient enough to produce target proteins for ribosome display.

Equally important to the quality of the target protein is the DARPin library used for the selection. Here, we generated two libraries optimized for straightforward subcloning into viral vector packaging plasmids. Each DARPin library covered at least 10^{12} DARPin molecules with the expected amino acid sequence and diversified positions confirming their high quality. DARPins active as targeting ligands were successfully selected from these newly generated as well as established DARPin libraries. Notably, 13 of the 13 selected DARPins that bound GluA4 in ELISA assays also recognized GluA4 in its native conformation on cells, confirming the quality of the target proteins.

It was previously shown for a panel of well-established Her2-specific DARPins that not all DARPins active in binding to a particular target

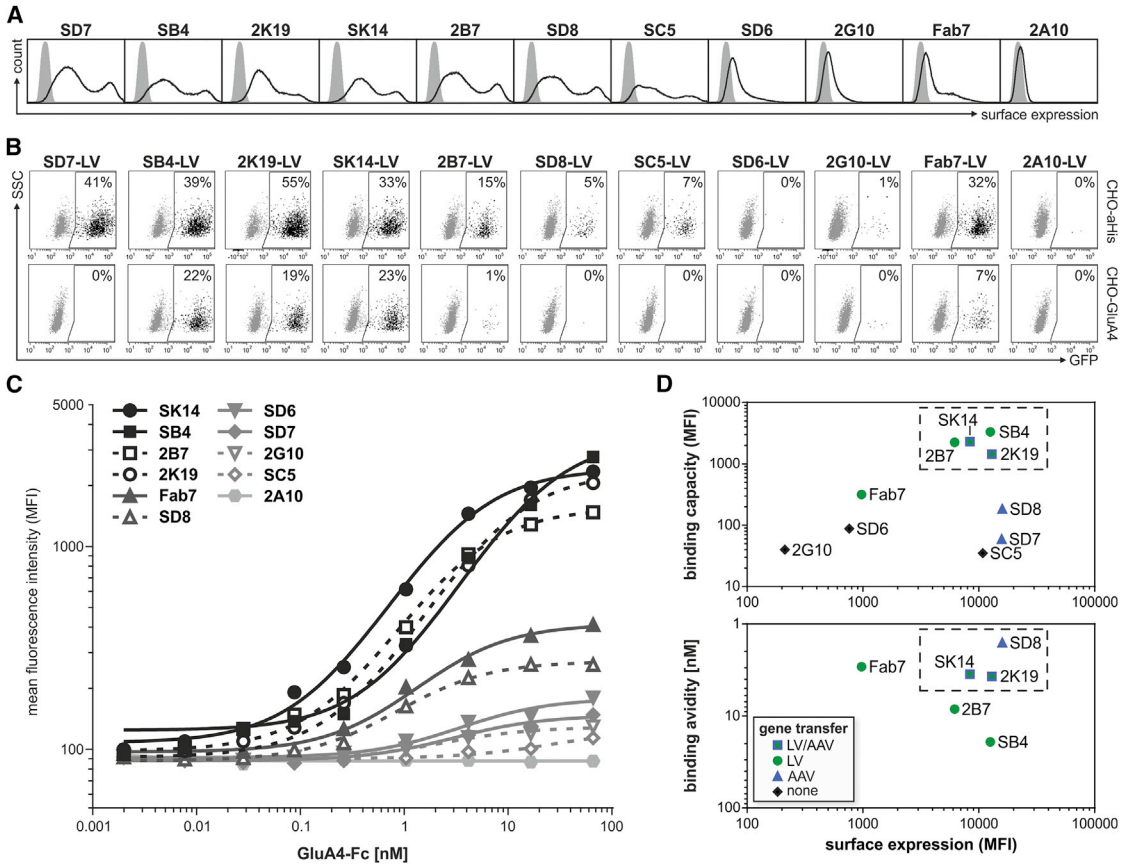

Figure 7. Correlation of the Binding and Surface-Expression Properties of the Selected GluA4-DARPins with Their Ability to Mediate Transduction

(A) Representative flow cytometry histograms showing the cell surface expression of GluA4-DARPin variants as indicated or the scFv Fab7 fused to the measles virus H protein after transient transfection of HEK293T cells with the corresponding expression plasmids (black lines) compared to mock-transfected cells (filled curves). (B) Transduction of CHO-αHis or CHO-GluA4 cells with DARPin-LV or Fab7-LV particles. Cells were analyzed for GFP expression 72 hr post-transduction by flow cytometry. The dot plots shown are representative for three biological replicas. The percentage of GFP-positive cells is indicated. (C) Binding of increasing amounts of recombinant GluA4-Fc protein to HEK293T cells expressing DARPin-H constructs as indicated or the Fab7-H protein on their surface. The mean fluorescence intensities (MFIs) of GluA4-Fc binding for the complete cell population are plotted against the concentration of GluA4-Fc applied for binding. Data were fitted to a 1:1 Langmuir binding model to determine apparent binding avidity and maximal functional binding values. (D) Correlation of surface expression and GluA4 binding properties of DARPin-H fusion proteins with the DARPin's ability to mediate gene transfer. MFIs of stained cell population as shown in (A) are plotted against the maximal functional binding capacity (top) or apparent binding avidity (bottom) as determined from curves shown in (C). Symbols indicate whether the DARPin enabled GluA4-targeted gene transfer for LVs and AAVs, only one of both, or none. The dashed lines indicate gates for the clustering of DARPins. See also Figures S8 and S9.

receptor mediate gene delivery by LVs equally well.[18] Accordingly, we set up a screening platform enabling the production of receptor-targeted LV and AAV vectors in a small-scale format, in order to identify those DARPins that mediate the most efficient viral gene transfer. Importantly, non-concentrated viral vector supernatant was used to indirectly assess in addition the influence of the DARPins on vector assembly and production yield. In this respect, we could recently demonstrate that ratios of VP1, VP2, and VP3 in assembled AAV capsids can vary with the polypeptide fused to VP2 and affect the overall yield.[35] Also for LV particles the DARPin can impact on the incorporation efficiency of the MV H fusion protein with a direct consequence for the overall amount of transduction-competent particles (Figures S9A and S9B).[18] Interestingly, less than half of the selected GluA4-DARPins and about one-third of the tested CD105-DARPins mediated gene transfer of LV or AAV vectors. Only two GluA4-DARPins (SK14 and 2K19) mediated efficient and specific transduction for both vector platforms. In contrast, the GluA4-binding DARPins SD7 and SD8 mediated gene transfer by AAV but not by LV. Notably, SK14, SD7, and SD8 exhibited very similar binding characteristics to GluA4 as tested from crude *E. coli* lysates and showed comparable surface expression when fused to the MV H protein. However, for DARPin candidates SD7 and SD8, the ability to bind to GluA4 got lost upon fusion to MV H, suggesting that target binding by these DARPins is either incompatible with their C-terminal fusions or they may become inactive through post-translational modifications such as glycosylation interfering with target receptor recognition. For display on LV particles, DARPins are fused to envelope glycoproteins and therefore traffic through the secretory

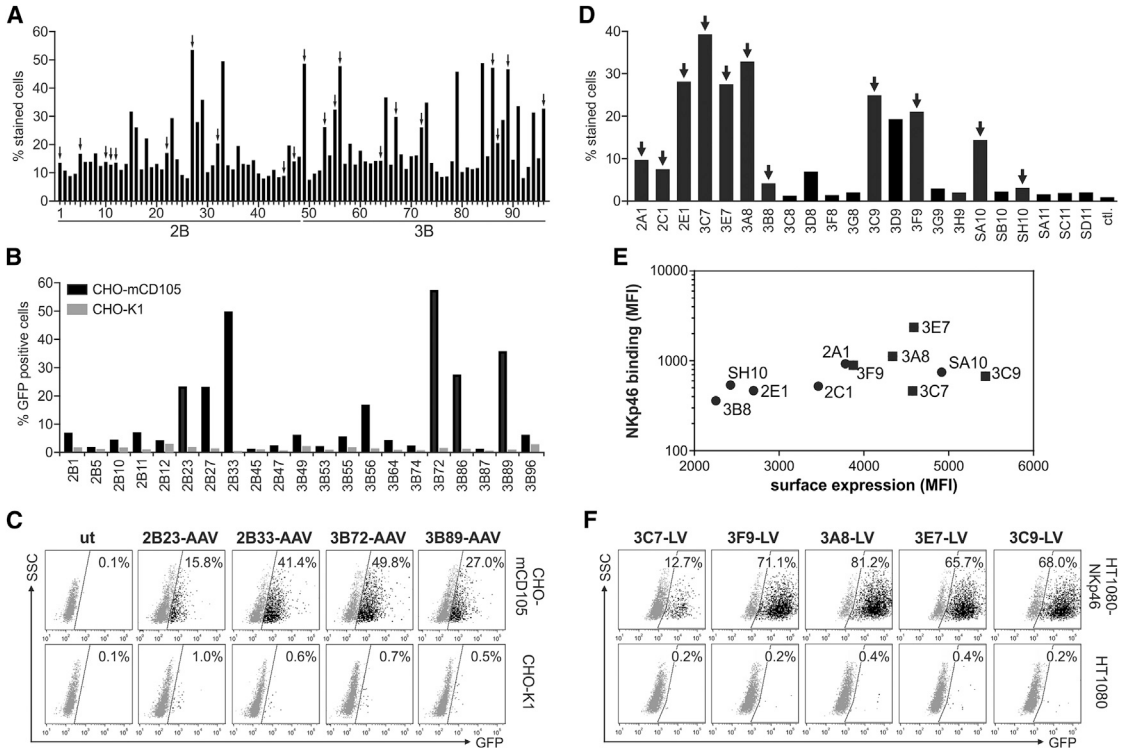

Figure 8. Selection of CD105 and NKp46-Specific DARPins for Receptor-Targeted Gene Transfer

B-N2C and B-N3C DARPin libraries were used to select binders specific for murine CD105 and DARPin libraries VV-N3C and S-N3C for the selection of binders specific for the NK cell marker NKp46. (A and D) Crude *E. coli* extracts of randomly picked clones obtained as output of the ribosomal display selection procedure for CD105 (A) and NKp46 (D) were analyzed for binding to HT1080 cells overexpressing the corresponding target receptor (HT1080-CD105, A; HT1080-NKp46, D) via flow cytometry. The percentage of cells bound by the DARPin clone is shown. Arrows indicate selected DARPins used for further analysis. For CD105, 96 (A) and for NKp46, 22 (D) individual *E. coli* extracts were analyzed. ctl, control *E. coli* extracts without DARPin. (B) 21 out of 96 identified CD105-binding DARPins were cloned into the expression plasmid pDARPin-VP2 and used to produce CD105-targeted AAV particles encoding GFP for transduction of CD105-positive (CHO-mCD105) and -negative (CHO-K1) cells. Cells were analyzed for GFP expression 72 hr post-transduction by flow cytometry. (C) Representative dot plots of four selected CD105-AAV particles from (B). The percentage of GFP-positive cells is indicated. ut, untransduced cells. (E) 11 identified NKp46-binding DARPins were cloned into the expression plasmid pCG-HΔ18-DARPin. Surface expression of the H-fusion proteins after transient transfection of HEK293T cells and binding of recombinant NKp46 were analyzed via flow cytometry. Correlation of the surface expression of the corresponding DARPin-H fusion protein and binding to recombinant NKp46 is shown. DARPins used for gene transfer experiments in (F) are indicated by rectangles. (F) HT1080-NKp46 and parental HT1080 cells were incubated with NKp46-DARPin displaying LV particles encoding GFP as indicated. Cells were analyzed 72 hr after transduction by flow cytometry. The percentage of GFP-positive cells is indicated.

pathway thus being exposed to the glycosylating enzymes of the ER and Golgi. In contrast, for re-targeting of AAV particles, DARPins are N-terminally coupled to the capsid protein VP2, which is a cytosolic protein, routed to the nucleus for AAV assembly. Thus, only DARPins used for LVs are exposed to glycosylation during transport to the cell surface.

Binding affinity is another important property of DARPins. To reflect the physiological situation of vector particle production and vector particle receptor interaction as close as possible, we decided to measure the binding of soluble receptors to cells transfected with expression plasmids encoding the DARPin-H fusion proteins. While the results from this assay may not be comparable to affinities determined by surface plasmon resonance (SPR), they provide at least relative values allowing us to better understand the binding requirements. Our analysis suggested that functional binding affinity appears to be more relevant for AAVs than for LVs. The lowest apparent avidity of DARPins compatible with AAV was 4 nM and 30 nM for those compatible with LV. An even lower affinity threshold of about 10^{-6} M has been previously determined for Her2-targeted MVs.[36,37] MV particles are larger than LV particles and likely contain more envelope proteins, thus potentially allowing compensation of lower affinities by higher avidity. Moreover, MVs are replication competent, and once cells have been entered mainly spread by cell-cell fusion, which can involve even more envelope protein receptor pairs.

For AAV, the situation is totally different. Only up to five DARPins can be displayed on a single AAV particle, which are at least 10-fold less than on LV.[15] In addition, entry pathways differ substantially: LV vectors rely on fusion at the cell membrane, while AAVs require endocytosis.[8] Receptor internalization is a rate-limiting

process and can vary between receptors. Cellular contact of AAV particles therefore has to outlast receptor internalization for efficient entry. In this respect, it will be important to determine if attachment of the DARPin to its receptor is sufficient or if secondary receptors like the recently identified AAVR are required in addition for cell entry of receptor re-targeted AAV vectors.[38] Interestingly, DARPin 2K19, which performed best on AAV, does not exhibit the highest functional binding affinity but, in contrast to all other DARPins, contains only a single diversified repeat. Such small ankyrin repeat proteins also occur naturally, although the majority possess two or three repeats.[39] They are likely better compatible with assembly and the packaging of genes into AAV particles considering that the DARPin likely extrude from the pores at the fivefold symmetry axis of the AAV capsid.[15] In order to still obtain sufficient affinity, such N1C DARPins typically have binding sites rich in hydrophobic and aromatic residues (J. Schaefer, M. Schmid, and A.P., unpublished data), which holds true for 2K19 as well (Figure S6).

GluA4, together with its closely related family members GluA1–3, belongs to the AMPA (α-amino-3-hydroxy-5-methylisoxazole-4-propionic acid) receptors and can form homo- as well as heteromers.[29] Inhibitory interneurons preferentially express GluA1 and GluA4, while GluA1 and GluA2 are present on excitatory neurons, at least in forebrain areas.[40] Therefore, exclusive recognition of GluA4 is required to target interneurons via AMPA receptors. Notably, AMPA receptors share up to 90% sequence identity within their LBDs and around 55% among their ATDs.[41] From the selection of phage-encoded antibodies against full-length GluA4 in proteoliposomes, it is known that cross-specific binders frequently occur.[42] All selected GluA4-DARPins enabling gene transfer by LV or AAV vectors were highly specific for GluA4, showing no measurable cross reactivity with the other AMPA family members. Interestingly, DARPin SK14 showed some binding to GluA2, however, only when purified protein from *E. coli* was tested. Its affinity for GluA2 thus seems to be too low, however, to result in off-target transduction.

In summary, the data presented in this manuscript imply that targeting ligands for LV and AAV vectors can be efficiently selected from DARPin libraries, when incorporating direct testing for gene delivery into the screening workflow. The data moreover show that, especially for AAV, the screening process on vector particles is important to identify those DARPins mediating the highest gene-delivery rates. This could suggest that, although technically challenging, cloning a (pre-selected) DARPin library directly into AAV could be a reasonable next step. The broad experience available with AAV peptide display and shuffled libraries will be helpful in this respect.[43,44] The selection and screening system we present here is highly flexible. This was demonstrated by the successful selection of DARPins specific for three different receptors. The novel generated GluA4-specific AAV and LV vectors will facilitate exploring the role of interneurons within the brain upon specific manipulation as well as gene therapy applications in epilepsy.[45] CD105-targeted AAVs may become applicable in tumor-targeted gene delivery,[46] and LVs targeted to NK cells via NKp46 could be applied in immunotherapy.[47]

MATERIALS AND METHODS

Plasmid Construction

To generate target proteins for ribosome display, the ATD of rat GluA4 (residues 22–401; amino acid positions refer to UniProt: P19493) was cloned in frame with the IgG signal peptide into the mammalian expression plasmid pCMV-hIgGI-Fc-XP,[48] providing a C-terminal human IgG-Fc region, to obtain pGluA4-huFc. To allow biotinylation of the protein, a C-terminal Avi tag was fused to the human IgG-Fc region behind a G_4S linker via PCR (primers 1 and 2). The PCR fragment was cloned into pGluA4-huFc and pCMV-hIgGI-Fc-XP via *Nhe*I and *Bcl*I to obtain pGluA4-huFc-Avi and phuFc-Avi, respectively. Plasmids encoding the extracellular domains of CD105 (residues 28–581; UniProt: Q63961) and NKp46 (residues 21–255; UniProt: O76036) were generated analogously to GluA4. Phusion High-Fidelity DNA polymerase (New England Biolabs, Frankfurt, Germany) was used for PCR reactions. All primer sequences for plasmid construction are available in Table S2.

To allow biotinylation of the Avi tag during protein expression within mammalian cells, the gene encoding for the BirA ligase was PCR amplified from *E. coli* TOP10 DNA. Primers 3 and 4 were used to obtain full-length BirA ligase behind a CMV promoter and an Ig kappa chain signal sequence and primers 3 and 5 to generate a BirA ligase additionally harboring a C-terminal ER retention signal consisting of the amino acids KDEL. Both PCR fragments were cloned into the mammalian expression plasmid pDisplay via *Xho*I and *Sfi*I to obtain pDisplay-sBirA and pDisplay-$BirA_{ER}$, respectively.

For analysis of selected DARPin binders, DARPin DNA fragments were cloned into the *E. coli* expression plasmid pQE-HisHA via *Sfi*I and *Dra*III containing an N-terminal $RGSHis_6$ tag followed by an HA tag. The plasmid pQE-HisHA was derived from pDST67[49,50] by oligo annealing of primers 6 and 7 as well as 8 and 9 and simultaneous insertion of the resulting two DNA fragments encoding for a His tag, HA tag, restrictions sites, and stop codons in pDST67 via *Eco*RI and *Pac*I. In addition, DNA fragments encoding the DARPin inserts were cloned into the mammalian expression plasmids pCG-HΔ18-DARPin encoding the blinded MV H-protein in fusion with a targeting domain and a C-terminal His tag,[51] and pDARPin-VP2 encoding a targeting domain in fusion with HSPG-blinded VP2 protein[15] via *Sfi*I and *Not*I. DARPins from the CD105 selection were cloned into the pDST67 expression plasmid via *Bam*HI and *Hind*III and PCR amplified (primers 10 and 11) as *Sfi*I and *Not*I fragments before cloning into pDARPin-VP2.

Cell Culture

HEK293T (ATCC CRL-11268), CHO-K1 (ATCC CCL-61), and HT1080 (ATCC CCL-121) cells were cultivated in DMEM (Sigma-Aldrich, Munich, Germany) supplemented with 10% fetal calf serum (FCS; Biochrom, Berlin, Germany) and 2 mM L-glutamine (Sigma-Aldrich, Munich, Germany). The cell lines CHO-GluA4, CHO-GluA1, CHO-GluA2, CHO-GluA3, CHO-GluR6, and CHO-αHis as well as CHO-CD105 were derived from CHO-K1 cells by LV

transduction (see below) and cultivated in the same medium in presence of 10 μg/mL (CHO-GluA4) or 2 μg/mL (CHO-GluA1-3, CHO-αHis) puromycin (Thermo Fisher Scientific, Darmstadt, Germany), or 1.2 mg/mL (CHO-mCD105) G418 (Thermo Fisher Scientific, Darmstadt, Germany). HT1080-NKp46 and HT1080-CD105 were derived from HT1080 cells and cultivated in the same medium in the presence of 400 μg/mL zeocin (InvivoGen, Toulouse, France) or 1.2 mg/mL G418, respectively. CHO-GluA4 cells were established by LV transduction of CHO-K1 cells with LV particles having packaged the coding sequence for GluA4 with an N-terminal myc tag.[13] For generation of CHO cells expressing glutamate receptor GluA1 (UniProt: P23818), GluA2 (UniProt: P19491), GluA3 (UniProt: P19492), or GluR6 (UniProt: P42260), the gene encoding for the corresponding glutamate receptor, including its native signal sequence in case of GluR6 or the signal sequence of uridine diphosphate (UDP)-glucosyltransferase in case of GluA1–3, was PCR amplified, thereby adding an N-terminal FLAG tag and cloned into a bicistronic LV transfer vector, encoding a spleen focus-forming virus (SFFV) promoter, an internal ribosome entry site (IRES) element followed by a puromycin resistance gene and a woodchuck posttranscriptional regulatory element (WPRE) via *Pac*I and *Spe*I, resulting in the bicistronic plasmids pS-GluA1-IPW, pS-GluA2-IPW, pS-GluA3-IPW, and pS-GluR6-IPW, respectively. CHO-GluA1, CHO-GluA2, CHO-GluA3, and CHO-GluA6 cells were established by LV transduction of CHO-K1 cells with LV particles having packaged the glutamate-receptor-encoding constructs. CHO-αHis cells were established by LV transduction of CHO-K1 cells with LV particles having packaged the coding sequence for the anti-His scFv 3D5[32] fused to the transmembrane region of the platelet-derived growth factor receptor (PDGFR). Transduced cells were selected using puromycin for 2 weeks. For the generation of HT1080 cells expressing NKp46, cells were transduced with LVs having packaging the full-length receptor in addition to the zeocin resistance marker. HT1080 and CHO cells expressing full-length CD105 were generated by transient transfection and selection with 1.2 mg/mL G418.[52]

Recombinant Protein Production and Purification

Target proteins for ribosome display were expressed in HEK293T cells by transient transfection using polyethylenimine (PEI) and purified from the cell culture medium. For direct biotinylation of the recombinant proteins during expression and after release into the cell culture supernatant, plasmids encoding for the target protein and pDisplay-sBirA and pDisplay-$BirA_{ER}$ were used in a ratio 1:2:2. Twenty-four hours before transfection, 1×10^7 cells were seeded per T175 flask. On the day of transfection, the cell culture medium was replaced by 10 mL DMEM with 15% FCS and 2 mM L-glutamine (DMEM + FCS). For the transfection mix, 35 μg of total DNA was mixed with 2.3 mL of DMEM without additives and added to 2.2 mL DMEM supplemented with 140 μL of 18 mM PEI solution. After incubation for 20 min at room temperature, the transfection mix was added to the HEK293T cells. 24 hr later, the medium was replaced by 20 mL DMEM supplemented with 5% Panexin NTA (Pan Biotech, Aidenbach, Germany) and 2 mM L-glutamine with or without 10 μM biotin per T175 flask. At day 2 post-transfection, cell supernatants containing the recombinant protein were passed through a 0.45-μm pore size filter and purified on Protein A-Sepharose (Thermo Fisher Scientific, Darmstadt, Germany) columns according to the manufacturer's recommendation. In brief, 200 μL of Protein A-Sepharose beads were incubated with 200 mL cell culture supernatant overnight at 4°C with shaking. On the next day, the beads were collected and washed with 20 mL PBS, before elution of the recombinant proteins with 5 mL of 100 mM glycine (pH 2.7). To neutralize the acidic pH, 1/10 volume of 1 M Tris (pH 8.8) was directly added to the eluted protein fractions. As a further polishing step, size-exclusion-chromatography was performed with the eluted recombinant proteins using a Superdex 200 HighLoad 16/600 column (GE Healthcare, Germany) in a high-pressure liquid chromatography (HPLC) system (ÄKTAxpress, GE Healthcare, Germany) according to the manufacturer's instructions using PBS as running buffer. Fractions containing the recombinant protein were pooled and concentrated using 50-kDa cut off spin concentrators. The concentrated protein was supplemented with 5% glycerol and protease inhibitor (cOmplete ULTRA, Roche, Mannheim, Germany) and stored at −80°C. Protein concentrations were determined by Bradford assay. For CD105, biotinylation was performed as previously described.[53]

Determination of Protein Biotinylation via ELISA

To determine the content of biotinylated GluA4-Fc protein within the protein preparation, 96-well Maxisorb plates (Nunc as part of Thermo Fischer Scientific, Darmstadt, Germany) were coated with graded amounts (0–44.6 pmol) of biotinylated and unbiotinylated GluA4-Fc and standard protein (MBP-Avitag fusion protein standard, BIS-300, Avidity, Aurora, Colorado, USA) in PBS. Coating was performed for 1 hr at room temperature. After washing the wells four times with 300 μL PBS-T (0.05% Tween 20 in PBS), unspecific binding was blocked by addition of 300 μL PBS-TB (0.5% BSA in PBS-T) per well for 1 hr at room temperature. Wells were washed four times with 300 μL PBS-T before incubation with horseradish peroxidase (HRP)-coupled streptavidin (1:500; 016-030-084, Jackson ImmunoResearch, West Grove, PA, USA) for 1 hr at room temperature. After washing the wells four times with PBS-T, the bound streptavidin was detected using SureBlue TMB substrate (KPL as part of SeraCare, Milford, MA, USA) and 1 N H_2SO_4. The reaction product was quantified in a microtiter plate reader at 450 nm.

DARPin Library Generation

The DARPin library was assembled repeat-by-repeat on the basis of previously described protocols.[20,21] In brief, a DNA library encoding one internal designed Ankyrin repeat diversified at seven amino acid positions as well as the constant N- and C-cap gene fragments were codon optimized for expression in *E. coli* and *de novo* synthesized by GeneArt. The DNA and amino acid sequence of the *de novo* synthesized DNA fragments is available in Table S3 and Figure S1A, respectively. The consensus sequence of the internal repeat and capping fragments was previously described.[23] In the first assembly step, the N-cap and the internal repeat, were digested using the type II restriction enzymes *Bsa*I and *Bbs*I, respectively, ligated, gel

purified, and PCR amplified (primers 1 and 2). Vent DNA Polymerase (New England Biolabs, Frankfurt, Germany) was used for PCR reactions. All primer sequences for DARPin library generation are available in Table S4. The purified PCR product was used as starting material for the next assembly round with another internal repeat. After the addition of two or three internal repeats to the N-cap fragment, the DARPin library was finalized by ligation of the C-cap fragment, PCR amplification (primers 3 and 4) and gel purification, resulting in a high-quality N2C and N3C DARPin library encoding approximately 1.8×10^{13} and 1.4×10^{13} diversified DARPin molecules, respectively. In a last step, the DARPin libraries were N-terminally flanked with a T7 Promoter, a ribosomal binding site, and a His tag, and C-terminally with a spacer sequence derived from TolA to allow *in vitro* transcription and the formation of a ternary complex of mRNA, ribosome, and the DARPin protein. The N- and C-terminal fragments were generated by PCR (primers 4 and 5; primers 7 and 8) using the pRDV plasmid as template.[54] After restriction of the N-terminal fragment with *Sfi*I, the C-terminal fragment with *Dra*III and the DARPin library with *Sfi*I and *Dra*III, the three fragments were ligated, gel purified, and PCR amplified using primers 9 and 10. The purified PCR product was used as starting material for ribosome display. Diversity of the assembled library and of each intermediate product was estimated from the amount of ligated DNA recovered after gel purification before PCR amplification (Table S1).

Ribosome Display

Ribosome display selections were carried out as previously described with some modification as indicated.[53] In brief, each ribosome display selection started with the coupled transcription and translation of DARPin libraries using the PURExpress *in vitro* synthesis kit (New England Biolabs, Frankfurt, Germany). For one coupled transcription and translation reaction, up to 100 ng DNA, 4 µL solution A, 3 µL solution B, and 0.4 µL RiboLock were incubated for 2 hr at 37°C in a total volume of 10 µL before adding 225 µL STOP mix (50 mM Tris-Ac [pH 7.5], 150 mM NaCl, 50 mM MgAc, 2.5 mg/mL heparin, 50 µg/mL *Saccharomyces cerevisiae* RNA). The produced ternary complexes of RNA, ribosomes, and DARPin proteins were subsequently subjected to pre-panning steps with 20 µM immobilized neutravidin or streptavidin per well as well as 20 µM immobilized recombinant Fc protein before being co-incubated with 40 µM of immobilized target proteins. After washing away non-binders, the bound ternary complexes were eluted and the purified mRNA (RNeasy Mini Kit; QIAGEN, Hilden, Germany) reverse transcribed using the AffinityScript Multiple Temperature Reverse Transcriptase (Agilent, Santa Clara, CA, USA) for 60 min at 50°C after primer annealing for 5 min at 95°C. The resulting DARPin DNA pool was amplified using primers 3 and 4 for the VV-N2C and VV-N3C libraries and primers 11 and 12 for the S-N3C library, flanked with N- and C-terminal fragments as described above and used as starting material for the next round of ribosome display. After three selection rounds on immobilized target proteins, two off-rate selection rounds with target in solution were performed using 6.5 pmol of biotinylated GluA4-Fc or Fc protein and 65 pmol of unbiotinylated GluA4-Fc protein. After the last selection round, DNA fragments encoding DARPin inserts were subjected to single clone-screening assays (see below). For the selection of CD105-specific DARPins, a separate transcription and translation reaction as well as error-prone PCR were performed using the N2C and N3C DARPin libraries, here termed B-N2C and B-N3C, described by Binz et al.[20], according to previously published protocols.[53]

Crude *E. coli* Extracts and Sequence Analysis

Single selected DARPins were expressed in 96-deep-well plates as described before with the exception that the expression vector pQE-HisHA was used instead of pDST67 for GluA4 and NKp46 selected DARPins.[50,53] In brief, DNA fragments encoding the DARPin inserts were subcloned into the expression vector pQE-HisHA via *Sfi*I and *Dra*III and used for transformation of *E. coli* XL1-blue bacteria. For screening of single clones, randomly picked colonies were subjected to DNA sequencing using standard techniques and used to inoculate 600 µL 2YT expression medium (2YT, 1% glucose, 100 µg/mL ampicillin) at 37°C. On the next day, 900 µL fresh 2YT expression medium was inoculated with 100 µL overnight culture for 1 hr at 37°C before addition of 100 µL of 5.5 mM isopropyl-β-D-thiogalactopyranosid (IPTG) in 2YT medium to each well and subsequent incubation at 37°C for 5 hr. All liquid cultures were incubated with shaking. After harvest by centrifugation, bacteria pellets were stored at −80°C. Thawed bacteria pellets were resuspended in 50 µL B-PER II (Thermo Scientific, Dreieich, Germany) before incubation at room temperature for 2 hr on an orbital shaker. After addition of 450 µL Tris-buffered saline (TBS) per well, cell debris was removed from crude extract by centrifugation. Crude extracts were aliquoted and stored at −80°C.

Small-Scale Purification of DARPins

E. coli XL-1 blue bacteria (Stratagene, San Diego, CA, USA) were transformed with pQE-HisHA plasmids containing selected DARPins. A single colony was used to inoculate 6 mL lysogeny broth (LB) expression medium (LB, 1% glucose, 100 mg/L ampicillin) at 30°C. On the next day, 5 mL overnight culture was used to inoculate 100 mL LB expression medium at 37°C. At an optical density (OD A_{600}) of 0.7, the cultures were induced with 300 µM IPTG and incubated for 4 hr at 37°C. All liquid cultures were incubated with shaking. After harvest, cells were suspended in 4 mL lysis buffer (50 mM Tris [pH 8.0], 500 mM NaCl) before cell disruption was performed by sonication for 4 min. After removal of cell debris by centrifugation at 17,000 × *g* for 15 min, lysis buffer was added to the cleared lysate to generate a total volume of 5 mL. Before purification of DARPins on Ni-nitrilotriacetic acid (NTA) Agarose (-QIAGEN, Hilden, Germany) columns according to the manufacturer, 3.5 mL 2.5× glycerol buffer (50 mM Tris [pH 8.0], 500 mM NaCl, 25% glycerol, 50 mM imidazole) was added to the lysates. Fractions containing the recombinant protein were pooled and dialyzed against PBS using 3.5 kDa molecular weight cut-off (MWCO) dialysis tubing. The dialyzed protein was supplemented with 5% glycerol and protease inhibitor (cOmplete ULTRA, Roche, Mannheim, Germany) and stored at −80°C. Protein concentration was determined by Bradford assay.

SDS-PAGE Analysis by Coomassie Staining and Western Blot

Proteins were incubated with 1× SDS-sample buffer (60 mM Tris [pH 6.8], 2% SDS, 10% glycerol, 5% β-mercaptoethanol, 0.015% bromophenol blue) at 95°C for 10 min and loaded on 10% or 15% SDS-PAGE gels as indicated. After electrophoretic separation, SDS-PAGE gels were either directly stained with PageBlue Protein Staining Solution (Thermo Fisher Scientific, Dreieich, Germany) according to the manufacturer, or proteins were blotted on nitrocellulose membranes.

The membranes were incubated with mouse anti-RGS-His_4 (1:1,000; 34650, QIAGEN, Hilden, Germany) and HRP conjugated rabbit anti-mouse (1:2,000; P0260, DAKO as part of Agilent, Santa Clara, CA) or HRP conjugated goat anti-human IgG (1:50,000; A0170, Sigma-Aldrich, Munich, Germany) or HRP conjugated streptavidin (1:5,000; 016-030-084, Jackson ImmunoResearch, West Grove, PA, USA). Signals were detected using the ECL Plus Western Blotting Detection System according to the manufacturer (Thermo Fisher Scientific, Dreieich, Germany). All antibodies were diluted in TBS-T (50 mM Tris, 150 mM NaCl, 0.1% Tween-20, pH 7.4) containing 2% powdered milk.

Vector Production

LV and AAV vector particles were generated by transient transfection using PEI as described above. In brief, 24 hr prior to transfection, 4×10^5 HEK293T cells were seeded per 12-well. On the day of transfection, the cell culture medium was replaced by 400 µL DMEM + FCS. For the transfection mix, 802 ng of total DNA was mixed with 53 µL of DMEM without additives and added to 50 µL DMEM supplemented with 3 µL of 18 mM PEI solution per 12-well plate. After incubation for 20 min at room temperature, the transfection mix was added to the HEK293T cells. 24 hr later, the medium was replaced by 750 µL fresh cell culture medium. At day 2 post-transfection, cell supernatants containing the vector particles were collected and centrifuged for 5 min at 1,000 × *g* to remove cell debris. The vector stocks were stored at 4°C (LV vector stocks max. 1 day; AAV vector stock max. 2 weeks).

For LV-targeting vectors, 30.9 ng of pCG-HΔ18-DARPin plasmid, 92.5 ng of pCG-FcΔ30 plasmid encoding MV F protein,[55] 331.0 ng of the packaging plasmid pCMVΔR8.9,[56] and 347.6 ng transfer vector pSEW encoding GFP as reporter[57] were used for transfection. LV particles pseudotyped with the vesicular stomatitis virus glycoprotein (VSV-G) were produced by co-transfection of 140.4 ng pMD.G2[58] along with 260.7 ng pCMVΔR8.9 and 401.0 ng pSEW.

AAV-targeting vectors and AAV-2 were generated using the adenovirus-helper-free AAV-packaging strategy.[59] For AAV-targeting vectors, 401.0 ng of the helper plasmid pXX6-80, 133.7 ng of the pRCVP2koA plasmid encoding *rep* and *cap* proteins of AAV-2 deleted for HSPG binding and mutated VP2 start codon,[15] 133.7 ng of the pDARPin-VP2 plasmid, and 133.7 ng of the self-complementary transfer vector pscGFP encoding GFP as reporter[14] were transfected. AAV-2 vector particles were produced by co-transfection of 481.2 ng pXX6-80 plasmid, 160.4 ng of the pRC plasmid encoding *rep* and *cap* proteins of AAV-2[60], and 160.4 ng pscGFP.

Transduction of Cell Lines and Flow Cytometry Analysis

For transduction, 3×10^8 cells of indicated cell lines were seeded into a single well of a 96-well plate. Twenty-four hours later, the cell culture medium was exchanged by 50 µL targeting-vector stock per well. After 2 hr, 150 µL cell culture medium was added per well. VSV-G-LVs and AAV-2 vectors were 1:50 and 1:5 diluted in 50 µL cell culture medium, respectively, prior to cell transduction. At day 3 post-transduction, transduced cells were determined by flow cytometry analysis based on the indicated percentage of green fluorescent cells. Flow cytometry analysis was performed on the MACSQuant Analyzer 10 (Miltenyi Biotec, Bergisch Gladbach, Germany). Data were analyzed using FCS Express version 4.0 (DeNovo Software).

Binding Assays and Surface Expression

For binding experiments of crude DARPin extracts as well as purified DARPins to target-positive and -negative cells, 1×10^5 cells were washed twice with FACS washing buffer (PBS, 2% FCS, 0.1% NaN_3) before incubation with 10 µL crude DARPin extracts or 5 µg of purified DARPin proteins for 1 hr at 4°C, respectively. After two additional washing steps, cells were stained with an Alexa 488-labeled anti-PentaHis antibody (1:330; 35310, QIAGEN, Hilden, Germany) for 15 min at 4°C if crude DARPin extracts were used or with a phycoerythrin (PE)-labeled anti-HA antibody (1:100; 130-092-257, Miltenyi Biotec, Bergisch Gladbach, Germany) for 30 min at 4°C in the case of purified DARPins. Before flow cytometry analysis, cells were washed again and resuspended in 100 µL FACS fixation buffer (PBS, 1% formaldehyde).

To analyze the surface expression of DARPin constructs displayed as a fusion to MV H-protein and their binding to recombinant GluA4, HEK293T cells were transfected with the corresponding pCG-HΔ18-DARPin expression plasmid. After 48 hr, 1×10^5 transfected cells were washed twice with FACS washing buffer and either directly stained with a PE-labeled anti-His antibody (1:100; 130-092-691, Miltenyi Biotec, Bergisch Gladbach, Germany) for 30 min at 4°C to determine the DARPin-H surface expression or incubated with increasing amounts of recombinant GluA4-huFc proteins (0–70 nM recombinant protein in up to 1 mL buffer) for 60 min at 4°C and a fluorescein isothiocyanate (FITC)-labeled anti-human Fc antibody (1:100; 2043-02, SouthernBiotech, Birmingham, AL, USA) with two washing steps in between. At an estimated receptor density of up to 1×10^5 receptors molecules per transfected cell,[18] ligand depletion can be excluded for all dilutions up to 0.017 nM. After two additional washing steps, cells were resuspended in FACS fixation buffer and subjected to flow cytometry analysis. Apparent binding avidity and functional binding capacity values were determined by fitting the curves to a 1:1 Langmuir binding model using Prism 7 software (GraphPad). To determine the surface expression and binding capacity of selected NKp46-specific DARPins, they were expressed as H fusion protein in HEK293T cells and detected via the His tag or incubated with 5 µg recombinant NKp46, respectively.

Competition Assay

50 μL of targeted LV and AAV vectors as well as 1 μL VSV-G-LVs and 10 μL AAV-2 in a total volume of 50 μL were pre-incubated with 2.2 μg of recombinant GluRD-Fc, 1.1 μg of Fc protein, or 2 μL PBS for 1 hr at 4°C, respectively. Afterwards, CHO-GluA4 and CHO-K1 were transduced with pre-incubated vector stocks before GFP expression was analyzed after 72 hr by flow cytometry.

ELISA-Based Binding Assay

96-well Maxisorb plates (Nunc as part of Thermo Fisher Scientific, Dreieich, Germany) were coated with 100 μL 20 μM Neutravidin solution in TBS for 1 hr at room temperature. After washing the wells three times with 300 μL TBS-T, unspecific binding was blocked by addition of 300 μL TBS-TB for 1 hr at room temperature. To immobilize the target protein, wells were incubated with 70 ng of biotinylated GluA4-Fc protein for 1 hr at 4°C on an orbital shaker. After three additional washing steps, wells were incubated with graded amounts of DARPin proteins (0–10 pmol/well) for 1 hr at 4°C on an orbital shaker. At the used ligand concentrations and volumes, ligand depletion could be excluded for concentrations $\geq$25 nM. To quantify the amount of bound DARPin proteins, wells were subsequently incubated with a mouse anti-RGS-His_4 antibody (1:5,000; 34650, QIAGEN, Hilden, Germany) and an HRP conjugated rabbit anti-mouse antibody (1:2,000; P0260, DAKO as part of Agilent, Santa Clara, CA) for 1 hr at room temperature. The plates were washed three times with TBS-T before and after each antibody incubation step. The bound antibodies were detected using SureBlue TMB substrate (KPL as part of SeraCare, Milford, MA, USA) and 1 N H_2SO_4. The reaction product was quantified in a microtiter plate reader at 450 nm. The apparent binding affinity was determined by fitting the curves to a 1:1 Langmuir binding model using Prism 7 software (GraphPad).

Statistical Analysis

Statistical analyses were performed with Prism 7 software (GraphPad). Tests for statistical significance used the unpaired two-tailed Student's t test or one-way ANOVA (Tukey's multiple comparisons test) as indicated; p values less than 0.05 were considered significant.

SUPPLEMENTAL INFORMATION

Supplemental Information includes Supplemental Materials and Methods, nine figures, and four tables and can be found with this article online at https://doi.org/10.1016/j.omtm.2018.07.001.

AUTHOR CONTRIBUTIONS

J.H., R.C.M., R.-T.F., I.C.S., B.D., and W.S. designed and performed experiments. J.H., R.C.M., I.C.S., B.D., M.A.S., A.P., and C.J.B. evaluated data. M.A.S., J.K., and A.P. contributed protocols and reagents and to writing of the manuscript. J.H. and C.J.B. conceived and designed the study, acquired grants, supervised work, and wrote the manuscript.

CONFLICTS OF INTEREST

The authors declare that they have no conflict of interest.

ACKNOWLEDGMENTS

This work was supported by grants from the LOEWE Center for Cell and Gene Therapy Frankfurt funded by the Hessische Ministerium für Wissenschaft und Kunst (HMWK; funding reference number III L 5-518/17.004 (2013)) to J.H. and the Deutsche Forschungsgemeinschaft SPP 1665 to C.J.B. (BU1301/4-1). This work was funded by a Professorship of the Swiss National Science Foundation (PP00P3_144823 to M.A.S.).

REFERENCES

1. Kumar, S.R., Markusic, D.M., Biswas, M., High, K.A., and Herzog, R.W. (2016). Clinical development of gene therapy: results and lessons from recent successes. Mol. Ther. Methods Clin. Dev. *3*, 16034.

2. Powell, S.K., Rivera-Soto, R., and Gray, S.J. (2015). Viral expression cassette elements to enhance transgene target specificity and expression in gene therapy. Discov. Med. *19*, 49–57.

3. Lévy, C., Verhoeyen, E., and Cosset, F.-L. (2015). Surface engineering of lentiviral vectors for gene transfer into gene therapy target cells. Curr. Opin. Pharmacol. *24*, 79–85.

4. Büning, H., Huber, A., Zhang, L., Meumann, N., and Hacker, U. (2015). Engineering the AAV capsid to optimize vector-host-interactions. Curr. Opin. Pharmacol. *24*, 94–104.

5. Dreier, B., Honegger, A., Hess, C., Nagy-Davidescu, G., Mittl, P.R.E., Grütter, M.G., Belousova, N., Mikheeva, G., Krasnykh, V., and Plückthun, A. (2013). Development of a generic adenovirus delivery system based on structure-guided design of bispecific trimeric DARPin adapters. Proc. Natl. Acad. Sci. USA *110*, E869–E877.

6. Schmid, M., Ernst, P., Honegger, A., Suomalainen, M., Zimmermann, M., Braun, L., Stauffer, S., Thom, C., Dreier, B., Eibauer, M., et al. (2018). Adenoviral vector with shield and adapter increases tumor specificity and escapes liver and immune control. Nat. Commun. *9*, 450.

7. Waehler, R., Russell, S.J., and Curiel, D.T. (2007). Engineering targeted viral vectors for gene therapy. Nat. Rev. Genet. *8*, 573–587.

8. Buchholz, C.J., Friedel, T., and Büning, H. (2015). Surface-Engineered Viral Vectors for Selective and Cell Type-Specific Gene Delivery. Trends Biotechnol. *33*, 777–790.

9. Yang, L., Bailey, L., Baltimore, D., and Wang, P. (2006). Targeting lentiviral vectors to specific cell types in vivo. Proc. Natl. Acad. Sci. USA *103*, 11479–11484.

10. Morizono, K., Xie, Y., Ringpis, G.-E., Johnson, M., Nassanian, H., Lee, B., Wu, L., and Chen, I.S. (2005). Lentiviral vector retargeting to P-glycoprotein on metastatic melanoma through intravenous injection. Nat. Med. *11*, 346–352.

11. Enkirch, T., Kneissl, S., Hoyler, B., Ungerechts, G., Stremmel, W., Buchholz, C.J., and Springfeld, C. (2013). Targeted lentiviral vectors pseudotyped with the Tupaia paramyxovirus glycoproteins. Gene Ther. *20*, 16–23.

12. Anliker, B., Abel, T., Kneissl, S., Hlavaty, J., Caputi, A., Brynza, J., Schneider, I.C., Münch, R.C., Petznek, H., Kontermann, R.E., et al. (2010). Specific gene transfer to neurons, endothelial cells and hematopoietic progenitors with lentiviral vectors. Nat. Methods *7*, 929–935.

13. Bender, R.R., Muth, A., Schneider, I.C., Friedel, T., Hartmann, J., Plückthun, A., Maisner, A., and Buchholz, C.J. (2016). Receptor-Targeted Nipah Virus Glycoproteins Improve Cell-Type Selective Gene Delivery and Reveal a Preference for Membrane-Proximal Cell Attachment. PLoS Pathog. *12*, e1005641.

14. Münch, R.C., Muth, A., Muik, A., Friedel, T., Schmatz, J., Dreier, B., Trkola, A., Plückthun, A., Büning, H., and Buchholz, C.J. (2015). Off-target-free gene delivery by affinity-purified receptor-targeted viral vectors. Nat. Commun. *6*, 6246.

15. Münch, R.C., Janicki, H., Völker, I., Rasbach, A., Hallek, M., Büning, H., and Buchholz, C.J. (2013). Displaying high-affinity ligands on adeno-associated viral vectors enables tumor cell-specific and safe gene transfer. Mol. Ther. *21*, 109–118.

16. Ungerechts, G., Engeland, C.E., Buchholz, C.J., Eberle, J., Fechner, H., Geletneky, K., Holm, P.S., Kreppel, F., Kühnel, F., Lang, K.S., et al. (2017). Virotherapy Research in Germany: From Engineering to Translation. Hum. Gene Ther. *28*, 800–819.

17. Plückthun, A. (2015). Designed ankyrin repeat proteins (DARPins): binding proteins for research, diagnostics, and therapy. Annu. Rev. Pharmacol. Toxicol. *55*, 489–511.

18. Münch, R.C., Mühlebach, M.D., Schaser, T., Kneissl, S., Jost, C., Plückthun, A., Cichutek, K., and Buchholz, C.J. (2011). DARPins: an efficient targeting domain for lentiviral vectors. Mol. Ther. *19*, 686–693.

19. Stumpp, M.T., Binz, H.K., and Amstutz, P. (2008). DARPins: a new generation of protein therapeutics. Drug Discov. Today *13*, 695–701.

20. Binz, H.K., Stumpp, M.T., Forrer, P., Amstutz, P., and Plückthun, A. (2003). Designing repeat proteins: well-expressed, soluble and stable proteins from combinatorial libraries of consensus ankyrin repeat proteins. J. Mol. Biol. *332*, 489–503.

21. Seeger, M.A., Zbinden, R., Flütsch, A., Gutte, P.G.M., Engeler, S., Roschitzki-Voser, H., and Grütter, M.G. (2013). Design, construction, and characterization of a second-generation DARP in library with reduced hydrophobicity. Protein Sci. *22*, 1239–1257.

22. Kramer, M.A., Wetzel, S.K., Plückthun, A., Mittl, P.R.E., and Grütter, M.G. (2010). Structural determinants for improved stability of designed ankyrin repeat proteins with a redesigned C-capping module. J. Mol. Biol. *404*, 381–391.

23. Binz, H.K., Amstutz, P., Kohl, A., Stumpp, M.T., Briand, C., Forrer, P., Grütter, M.G., and Plückthun, A. (2004). High-affinity binders selected from designed ankyrin repeat protein libraries. Nat. Biotechnol. *22*, 575–582.

24. Plückthun, A. (2012). Ribosome display: a perspective. Methods Mol. Biol. *805*, 3–28.

25. Marín, O. (2012). Interneuron dysfunction in psychiatric disorders. Nat. Rev. Neurosci. *13*, 107–120.

26. Montaldo, E., Del Zotto, G., Della Chiesa, M., Mingari, M.C., Moretta, A., De Maria, A., and Moretta, L. (2013). Human NK cell receptors/markers: a tool to analyze NK cell development, subsets and function. Cytometry A *83*, 702–713.

27. Nassiri, F., Cusimano, M.D., Scheithauer, B.W., Rotondo, F., Fazio, A., Yousef, G.M., Syro, L.V., Kovacs, K., and Lloyd, R.V. (2011). Endoglin (CD105): a review of its role in angiogenesis and tumor diagnosis, progression and therapy. Anticancer Res. *31*, 2283–2290.

28. Parrott, M.B., and Barry, M.A. (2001). Metabolic biotinylation of secreted and cell surface proteins from mammalian cells. Biochem. Biophys. Res. Commun. *281*, 993–1000.

29. Traynelis, S.F., Wollmuth, L.P., McBain, C.J., Menniti, F.S., Vance, K.M., Ogden, K.K., Hansen, K.B., Yuan, H., Myers, S.J., and Dingledine, R. (2010). Glutamate receptor ion channels: structure, regulation, and function. Pharmacol. Rev. *62*, 405–496.

30. Sobolevsky, A.I., Rosconi, M.P., and Gouaux, E. (2009). X-ray structure, symmetry and mechanism of an AMPA-subtype glutamate receptor. Nature *462*, 745–756.

31. Stefan, N., Martin-Killias, P., Wyss-Stoeckle, S., Honegger, A., Zangemeister-Wittke, U., and Plückthun, A. (2011). DARPins recognizing the tumor-associated antigen EpCAM selected by phage and ribosome display and engineered for multivalency. J. Mol. Biol. *413*, 826–843.

32. Lindner, P., Bauer, K., Krebber, A., Nieba, L., Kremmer, E., Krebber, C., Honegger, A., Klinger, B., Mocikat, R., and Plückthun, A. (1997). Specific detection of his-tagged proteins with recombinant anti-His tag scFv-phosphatase or scFv-phage fusions. Biotechniques *22*, 140–149.

33. Pollack, S.M., Lu, H., Gnjatic, S., Somaiah, N., O'Malley, R.B., Jones, R.L., Hsu, F.J., and Ter Meulen, J. (2017). First-in-Human Treatment With a Dendritic Cell-targeting Lentiviral Vector-expressing NY-ESO-1, LV305, Induces Deep, Durable Response in Refractory Metastatic Synovial Sarcoma Patient. J. Immunother. *40*, 302–306.

34. Barat, B., and Wu, A.M. (2007). Metabolic biotinylation of recombinant antibody by biotin ligase retained in the endoplasmic reticulum. Biomol. Eng. *24*, 283–291.

35. Muik, A., Reul, J., Friedel, T., Muth, A., Hartmann, K.P., Schneider, I.C., Münch, R.C., and Buchholz, C.J. (2017). Covalent coupling of high-affinity ligands to the surface of viral vector particles by protein trans-splicing mediates cell type-specific gene transfer. Biomaterials *144*, 84–94.

36. Hasegawa, K., Hu, C., Nakamura, T., Marks, J.D., Russell, S.J., and Peng, K.-W. (2007). Affinity thresholds for membrane fusion triggering by viral glycoproteins. J. Virol. *81*, 13149–13157.

37. Suksanpaisan, L., Russell, S.J., and Peng, K.-W. (2014). High scFv-receptor affinity does not enhance the antitumor activity of HER2-retargeted measles virus. Cancer Gene Ther. *21*, 256–260.

38. Pillay, S., Meyer, N.L., Puschnik, A.S., Davulcu, O., Diep, J., Ishikawa, Y., Jae, L.T., Wosen, J.E., Nagamine, C.M., Chapman, M.S., and Carette, J.E. (2016). An essential receptor for adeno-associated virus infection. Nature *530*, 108–112.

39. Mosavi, L.K., Cammett, T.J., Desrosiers, D.C., and Peng, Z.-Y. (2004). The ankyrin repeat as molecular architecture for protein recognition. Protein Sci. *13*, 1435–1448.

40. Fuchs, E.C., Zivkovic, A.R., Cunningham, M.O., Middleton, S., Lebeau, F.E.N., Bannerman, D.M., Rozov, A., Whittington, M.A., Traub, R.D., Rawlins, J.N., and Monyer, H. (2007). Recruitment of parvalbumin-positive interneurons determines hippocampal function and associated behavior. Neuron *53*, 591–604.

41. Furukawa, H. (2012). Structure and function of glutamate receptor amino terminal domains. J. Physiol. *590*, 63–72.

42. Jespersen, L.K., Kuusinen, A., Orellana, A., Keinänen, K., and Engberg, J. (2000). Use of proteoliposomes to generate phage antibodies against native AMPA receptor. Eur. J. Biochem. *267*, 1382–1389.

43. Grimm, D., and Büning, H. (2017). Small But Increasingly Mighty: Latest Advances in AAV Vector Research, Design, and Evolution. Hum. Gene Ther. *28*, 1075–1086.

44. Bartel, M.A., Weinstein, J.R., and Schaffer, D.V. (2012). Directed evolution of novel adeno-associated viruses for therapeutic gene delivery. Gene Ther. *19*, 694–700.

45. Wykes, R.C., and Lignani, G. (2018). Gene therapy and editing: Novel potential treatments for neuronal channelopathies. Neuropharmacology *132*, 108–117.

46. Dallas, N.A., Samuel, S., Xia, L., Fan, F., Gray, M.J., Lim, S.J., and Ellis, L.M. (2008). Endoglin (CD105): a marker of tumor vasculature and potential target for therapy. Clin. Cancer Res. *14*, 1931–1937.

47. Guillerey, C., Huntington, N.D., and Smyth, M.J. (2016). Targeting natural killer cells in cancer immunotherapy. Nat. Immunol. *17*, 1025–1036.

48. Friedel, T., Hanisch, L.J., Muth, A., Honegger, A., Abken, H., Plückthun, A., Buchholz, C.J., and Schneider, I.C. (2015). Receptor-targeted lentiviral vectors are exceptionally sensitive toward the biophysical properties of the displayed single-chain Fv. Protein Eng. Des. Sel. *28*, 93–106.

49. Huber, T., Steiner, D., Röthlisberger, D., and Plückthun, A. (2007). In vitro selection and characterization of DARPins and Fab fragments for the co-crystallization of membrane proteins: The Na(+)-citrate symporter CitS as an example. J. Struct. Biol. *159*, 206–221.

50. Steiner, D., Forrer, P., and Plückthun, A. (2008). Efficient selection of DARPins with sub-nanomolar affinities using SRP phage display. J. Mol. Biol. *382*, 1211–1227.

51. Funke, S., Maisner, A., Mühlebach, M.D., Koehl, U., Grez, M., Cattaneo, R., Cichutek, K., and Buchholz, C.J. (2008). Targeted cell entry of lentiviral vectors. Mol. Ther. *16*, 1427–1436.

52. Abel, T., El Filali, E., Waern, J., Schneider, I.C., Yuan, Q., Münch, R.C., Hick, M., Warnecke, G., Madrahimov, N., Kontermann, R.E., et al. (2013). Specific gene delivery to liver sinusoidal and artery endothelial cells. Blood *122*, 2030–2038.

53. Dreier, B., and Plückthun, A. (2012). Rapid selection of high-affinity binders using ribosome display. Methods Mol. Biol. *805*, 261–286.

54. Ng, D.T.W., and Sarkar, C.A. (2012). Model-guided ligation strategy for optimal assembly of DNA libraries. Protein Eng. Des. Sel. *25*, 669–678.

55. Funke, S., Schneider, I.C., Glaser, S., Mühlebach, M.D., Moritz, T., Cattaneo, R., Cichutek, K., and Buchholz, C.J. (2009). Pseudotyping lentiviral vectors with the

wild-type measles virus glycoproteins improves titer and selectivity. Gene Ther. *16*, 700–705.

56. Zufferey, R., Nagy, D., Mandel, R.J., Naldini, L., and Trono, D. (1997). Multiply attenuated lentiviral vector achieves efficient gene delivery in vivo. Nat. Biotechnol. *15*, 871–875.

57. Demaison, C., Parsley, K., Brouns, G., Scherr, M., Battmer, K., Kinnon, C., Grez, M., and Thrasher, A.J. (2002). High-level transduction and gene expression in hematopoietic repopulating cells using a human immunodeficiency [correction of imunodeficiency] virus type 1-based lentiviral vector containing an internal spleen focus forming virus promoter. Hum. Gene Ther. *13*, 803–813.

58. Salmon, P., and Trono, D. (2007). Production and titration of lentiviral vectors. Curr. Protoc. Hum. Genet. *54*, 12.10.1–12.10.24.

59. Xiao, X., Li, J., and Samulski, R.J. (1998). Production of high-titer recombinant adeno-associated virus vectors in the absence of helper adenovirus. J. Virol. *72*, 2224–2232.

OMTM, Volume *10*

Supplemental Information

A Library-Based Screening Strategy for the Identification of DARPins as Ligands for Receptor-Targeted AAV and Lentiviral Vectors

Jessica Hartmann, Robert C. Münch, Ruth-Therese Freiling, Irene C. Schneider, Birgit Dreier, Washington Samukange, Joachim Koch, Markus A. Seeger, Andreas Plückthun, and Christian J. Buchholz

Supplementary Figures

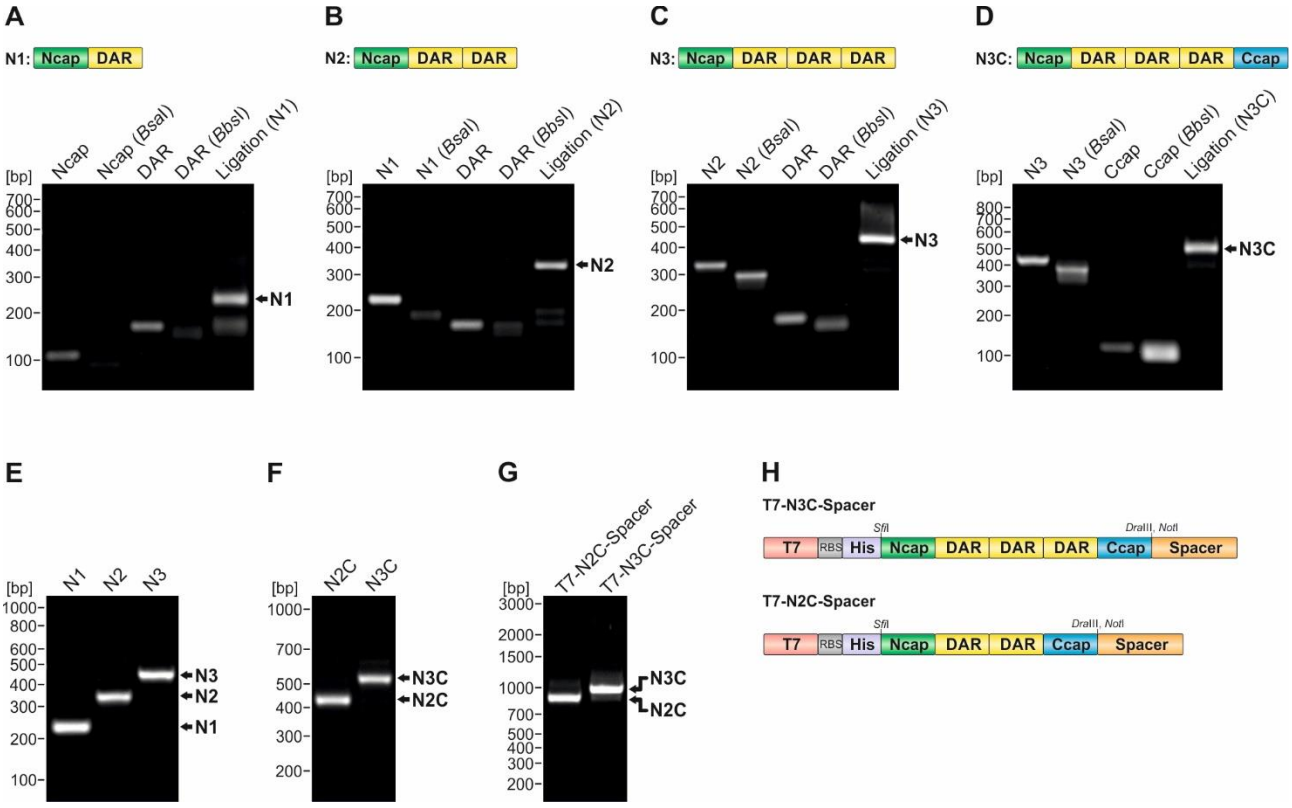

Figure S1: Stepwise generation of the VV-N2C and VV-N3C DARPin libraries.

DARPin libraries were assembled from DNA fragments encoding a constant N-terminal capping domain (Ncap), a constant C-terminal capping domain (Ccap) and diversified designed ankyrin repeat (DAR) elements generated with degenerated oligonucleotides. **(A-D)** 200 ng of the undigested and digested PCR fragments and the product of the ligation reaction, respectively, were separated on 2% agarose gels. A schematic drawing of the resulting DNA fragment of each assembly step is depicted above each gel. **(E-G)** Agarose gel analysis of purified DARPin DNA after PCR amplification of the corresponding ligation product. On a 2 % agarose gel 200 ng of DNA were separated and stained with ethidium bromide. **(H)** Schematic representation of the DARPin libraries. The N2C and N3C DARPin libraries are flanked by a T7 promoter (T7), a ribosome binding site (RBS) and a hexahistidin tag (His) as well as a spacer sequence encoding an unstructured region from the *E. coli* TolA protein without stop codon. Positions of the added restriction sites are indicated.

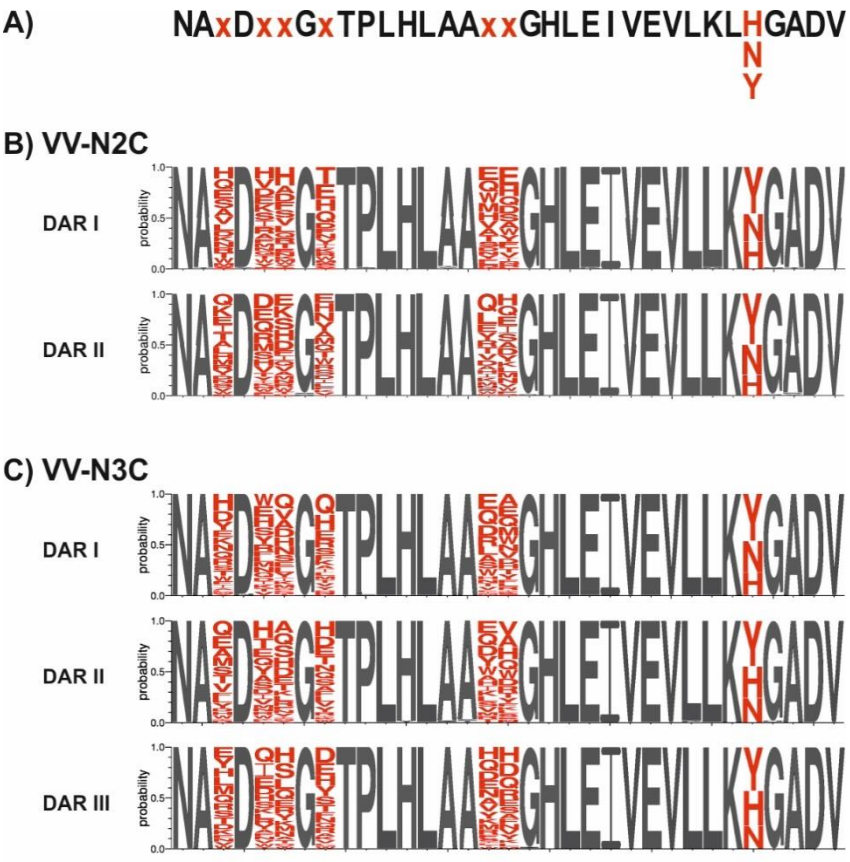

Figure S2: Sequence analysis of the generated DARPin libraries.

(A) Consensus sequence of one designed ankyrin repeat (DAR) element on protein level. Each DAR harbors six diversified positions (red x), where any amino acid is allowed except of glycine, proline or cysteine, and one diversified positions being a histidine, asparagine or tyrosine. **(B, C)** Sequence logo of the generated VV-N2C (B) and VV-N3C (C) DARPin library covering the DAR elements. To verify the frame work and diversified positions of the generated DARPin libraries, 45 ng of each library DNA was cloned into the plasmid pJet1.2 and transformed into *E. coli* TOP10. 100 individual clones per library were analyzed by sequencing. 76 (N2C) and 58 (N3C) sequences encoded a DARPin and were used to create the corresponding sequence logo using WebLogo 3 (http://weblogo.threeplusone.com/create.cgi).

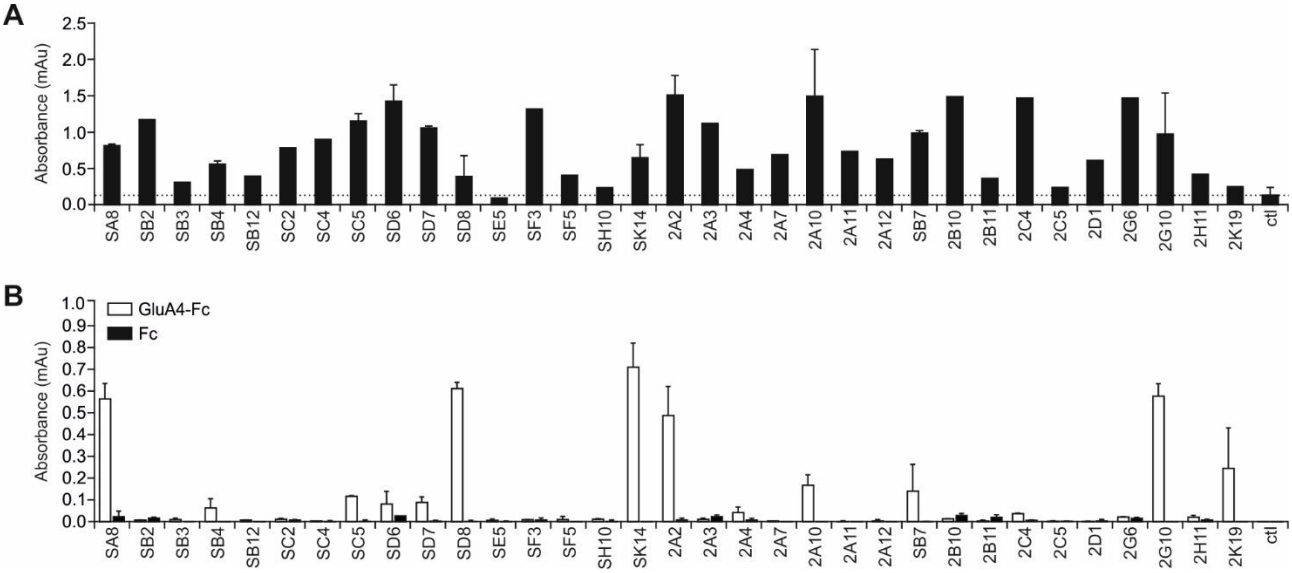

Figure S3: Screening and characterization of ribosome display selected GluA4-DARPins.

Crude *E. coli* extracts of randomly picked clones were analyzed for the expression of soluble DARPins (**A**) and tested for binding to recombinant GluA4-Fc (**B**) by ELISA. (**A**) 1 µl of crude *E. coli* extracts were coated on immunoplates. DARPins were detected using a biotinylated anti-His antibody in conjunction with HPR-conjugated streptavidin. (**B**) Recombinant GluA4-Fc or recombinant Fc protein was used to determine DARPins specific for GluA4 or the constant region of human IgG1 (huIgG1-Fc), which is present in the GluA4-Fc protein. DARPins were detected using an anti-His antibody in conjunction with a HRP-conjugated anti-mouse antibody.

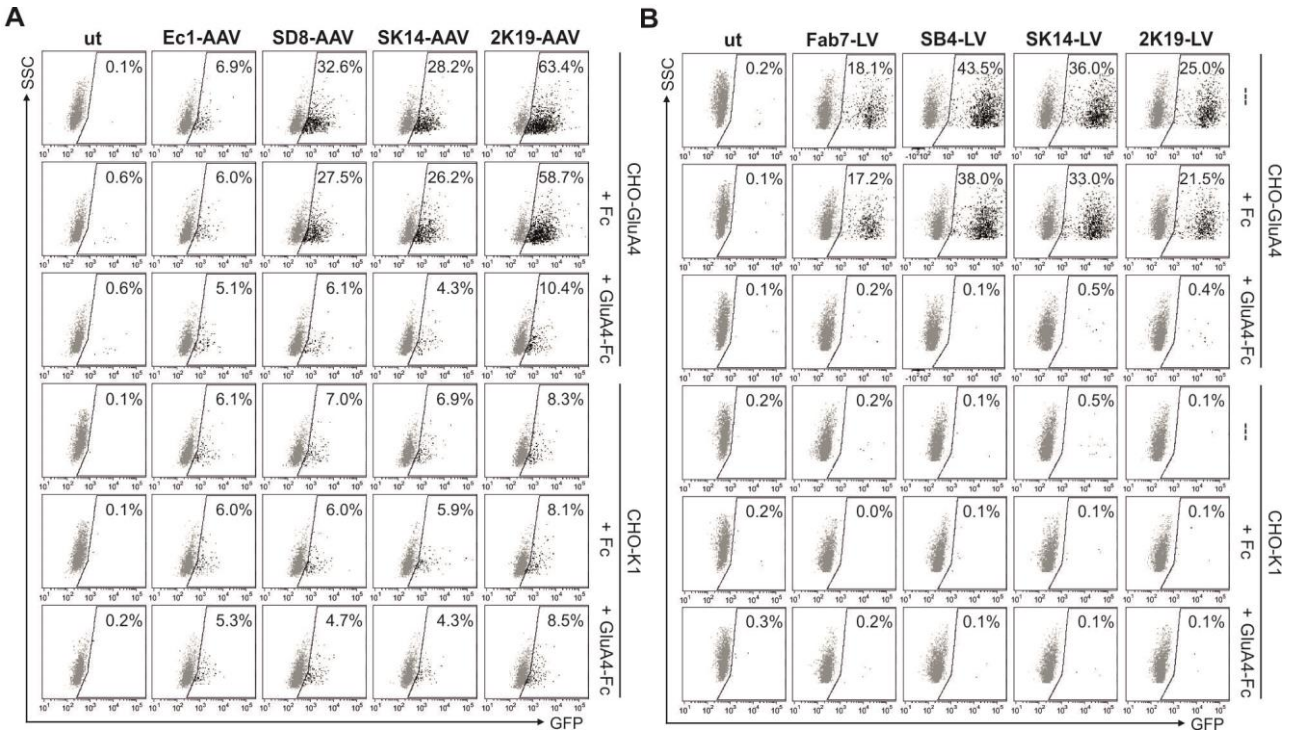

Figure S4: Competition assay evaluating DARPin mediated transduction.

For the best performing AAV (**A**) and LV (**B**) particles displaying the indicated DARPins a competition assay was performed by incubation of the vector particles with recombinant GluA4-Fc and Fc proteins, respectively or buffer as control prior to transduction of CHO-K1 or CHO-GluA4 cells. The cells were analyzed for GFP expression 72 h post transduction by flow cytometry. Untransduced cells and AAV particles displaying the EpCam-specific DARPin Ec1 were used as negative control. For LVs, particles displaying the scFv Fab7 were used as positive control. Unmodified AAV particles and VSV-G pseudotyped LV particles are used as control. Each transduction experiment was performed at least three times with individually produced vector particles, showing mean values and standard deviations (SD). Representative dot plots are shown. The percentage of GFP positive cells is indicated.

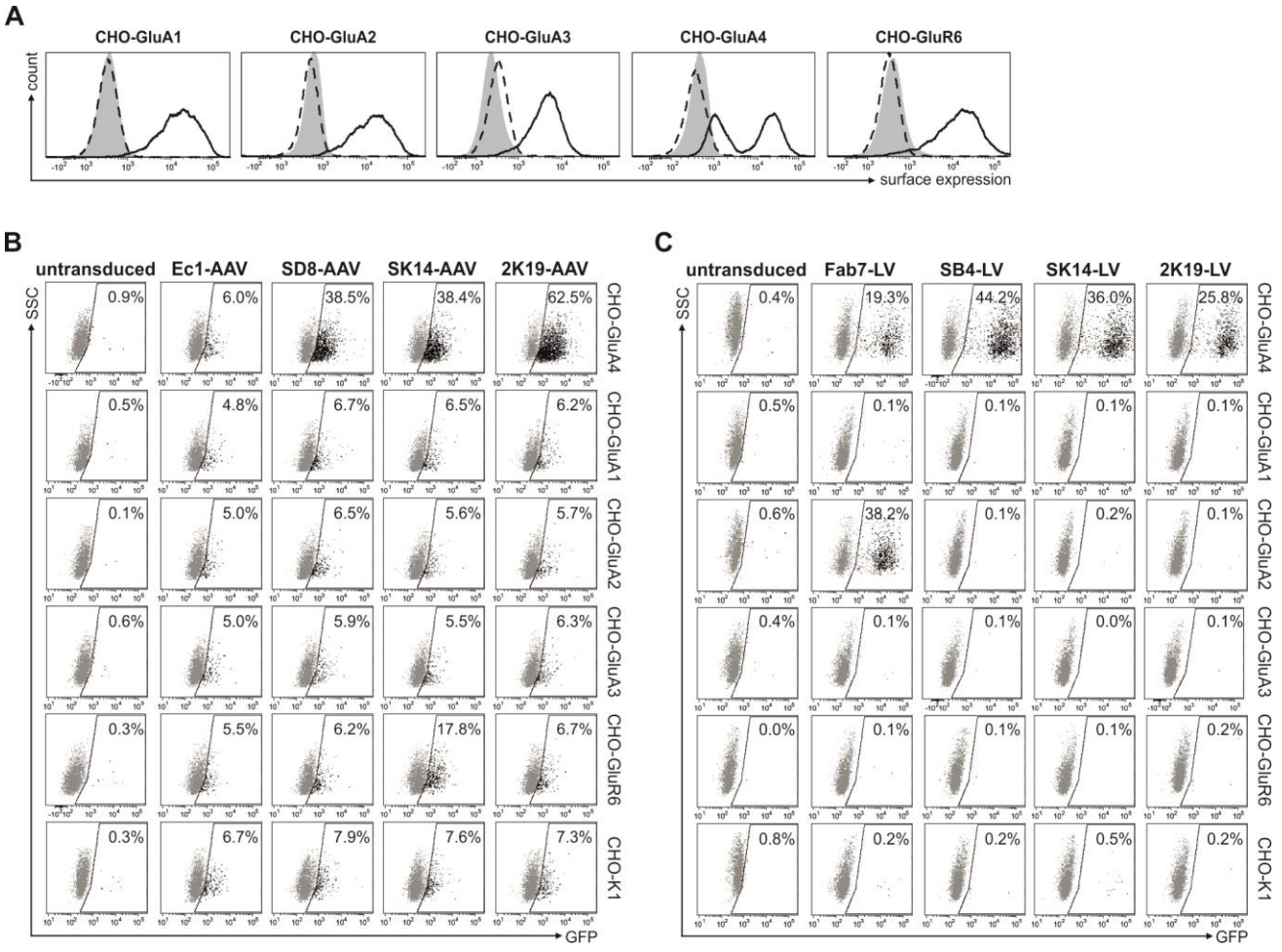

Figure S5: Transduction of a panel of CHO cells expressing various glutamate receptors.

(A) Representative flow cytometry histograms showing the cell surface expression of glutamate receptors as indicated after transduction of CHO-K1 cells with lentiviral vectors encoding the corresponding glutamate receptor. Cells were stained with a PE coupled myc tag specific antibody (solid black line) in the case of CHO-GluA4 cells and with a PE coupled Flag tag specific antibody (solid black line) in the case of CHO-GluA1, CHO-GluA2, CHO-GluA3 and CHO-GluR6 cells. As control cells were incubated with buffer only (filled curves) and compared to CHO-K1 cells stained with the respective fluorophore coupled antibody (dashed black lines). (**B-C**) CHO-K1 cells expressing GluA1-4 or GluR6 as well as the parental cell line were incubated with AAV (**B**) or LV (**C**) particles displaying the indicated DARPins. The cells were analyzed for GFP expression 72 h post transduction by flow cytometry. Untransduced cells and AAV particles displaying the EpCAM-specific DARPin Ec1 (**B**) or LV particles displaying the GluA2/4-specific scFv Fab7 (**C**) served as controls. Each transduction experiment was performed at least three times with individually produced vector particles, showing mean values and standard deviations. Representative dot plots are shown in the bottom panel. The percentage of GFP-positive cells is indicated.

A) S-N3C

```
     <------------------Ncap--------------------->|<------------AR1---------------->
SA8  MRGSHHHHHHAAQPAKDLGKKLLDAASAGQDDEVRILMANGADV|NASDWRGRTPLHAAAQKGHLEIVDVLLTHGADV
SB4  MRGSHHHHHHAAQPAKDLGKKLLDAASAGQDDEVRILMANGADV|NASDWRGRTPLHAAAQKGHLEIVDVLLAHGADV
SC5  MRGSHHHHHHAAQPAKDLGKKLLDAASAGQDDEVRILMANGADV|NASNWTGATPLHAAADWGHLEIVDVLLANGADV
SD6  MRGSHHHHHHAAQPAKDLGKKLLDAASAGQDDEVRILMANGADV|NASDWRGRTPLHAAAQKGHLEIVDVLLAHGADV
SD7  MRGSHHHHHHAAQPAKDLGKKLLDAASAGQDDEVRILMANGADV|NASDWRGRTPLHAAAQKGHLEIVDVLLAHGADV
SD8  MRGSHHHHHHAAQPAKDLGKKLLDAASAGQDDEVRILMANGADV|NASDWDGKTPLYLAARNGHLEIVDVLLAHGADV
SK14 MRGSHHHHHHAAQPAKDLGKKLLDAASAGQDDEVRILMANGADV|NASTWAGDTPLHLAARNGHLEIVDVLLAHGADV

     <------------AR2----------------->|<------------AR3----------------->|<-----------Ccap------------->
SA8  NASDHYGWTPLHTAAAYGHLEIVDVLLAHGADV|                                  |NANTYSGKTPFDLAIDNGNEDIAEVLQKAA
SB4  NASDSNGKTTLHVAAADGHLEIVDVLLANGADV|NASDHYGWTPLHTAAAYGHLEIVDVLLAHGADV|NANTYSGKTPFDLAIDNGNEDIAEVLQKAA
SC5  NASDTNGSTPLHAAASSGHLEIVDVLLANDADV|NASNHYGWTPLHTAASYGHLEIVDVLLAYGADV|NANTYSGKTPFDLAIDNGNEDIAEVLQKAA
SD6  NASDSNGKTTLHVAAADGHLEIVDVLLANGADV|NASNHYGWTPLHTAASYGHLEIVDVLLAYGADV|NANSYSGKTPFDLAIDNGNEDIAEVLQKAA
SD7  NASDTNGSTPLHAAASSGHLEIVDVLLANGADV|NASNHYGWTPLHTAASYGHLEIVDVLLAYGADV|NANTYSGKTPFDLAIDNGNEDIAEVLQKAA
SD8  NASDTNGSTPLHAAASSGHLEIVDVLLANGADV|NASNHYGWTPLHTAASYGHLEIVDVLLAYGADV|NANTYSGKTPFDLAIDNGNEDIAEVLQKAA
SK14 NASDTNGSTPLHAAASSGHLEIVDVLLANGADV|NASNHYGWTPLHTAAAWGHLEIVDVLLANGADV|NANSYSGKTPFDLAIDNGNEDIAEVLQKAA
```

B) VV-N2C

```
     <------------------Ncap--------------------->|<------------AR1---------------->
2A2  MRGSHHHHHHAAQPADLGKKLLEAARAGQDDEVRILMANGADV|NAQDWEGRTPLHLAAHNSHLEIVEVLLKHGADV
2A10 MRGSHHHHHHAAQPADLGKKLLEAARAGQDDEVRILMANGADV|NALDHWGTTPLHLAAWSGHLEIVEVLLKNGADV
2B7  MRGSHHHHHHAAQPADLGKKLLEAARVGQDDEVRILMANGADV|NANDYHGSTPLHLAADYGHLEIVEVLLKYGADV
2G10 MRGSHHHHHHAAQPADLGKKLLEAARAGQDDEVRILMANGADV|NAQDWEGRTPLHLAAHNSHLEIVEVLLKHGADV
2K19 MRGSHHHHHHAAQPADLGKKLLEAARAGQNDEVRILMANGADV|NAIDMAGRTPLHLAAWSGHLEIVEVLLKYDADV

     <------------AR2----------------->|<-----------Ccap------------->
2A2  NAFDWYGNTPLHQAAAQGHLEIVEVLLKYGEDV|NAQDKFGKTPFDLAIDNGNEDIAEVLQKAA
2A10 NATDYQGRTPLHLAAVMGHLEIVEVLLKNGADV|NAQDKFGKTPFDLAIDNGMKILPKCCRKQ
2B7  NALDNMGMTPLHLAAQWGHLEIVEVLLKNGADV|NAQDKFGKTPFDLAIDNGNEDIAEVLQKAA
2G10 NAFDWYGNTPLHQAAAQGHLEIVEVLLKYGEDV|NAQDKFGKTPFDLAIDNGNEDIAEVPESSA
2K19                                  |NATDHFGLTPLHLAASDGHLDIAEVLQKAA
```

Figure S6: Sequence alignment of 12 DARPins selected for GluA4 binding via ribosome display.

Sequence alignment of DARPin candidates selected from the S-N3C library (A) and the VV-N3C library (B). The amino acid sequence was determined by sequencing of the corresponding pQE plasmid DNA. The diversified positions are highlighted in bold. Color code indicates the amino acid (AA) property (red, small and hydrophobic AA including aromatic AA; blue, negatively charged AA; lilac, positively charged AA; green, polar AA including tyrosine and histidine). Point mutations within the framework regions are shown in italic-black.

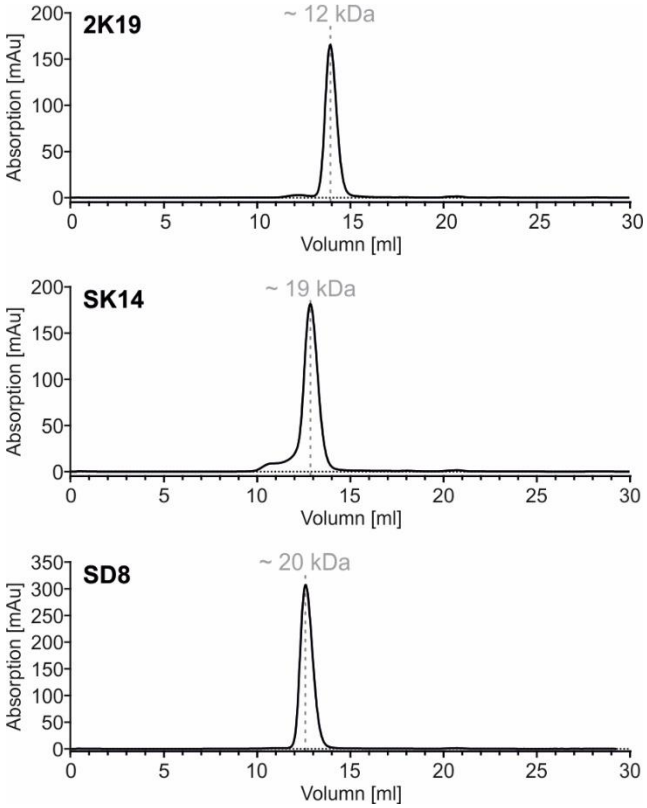

Figure S7: Size exclusion chromatography of purified DARPins.

Size exclusion chromatogram of the indicated DARPins expressed in *E. coli* and purified via His-tag affinity chromatography. The calculated molecular weight of the corresponding peak is indicated.

Figure S8: Binding of recombinant GluA4 to selected GluA4-DARPins.

Representative flow cytometry histograms obtained after transient transfection of HEK293T cells with expression plasmids encoding the fusion protein composed of H and the indicated DARPin. The Fab7-H fusion protein served as positive control. Transfected cells were either stained with a PE-coupled His-tag specific antibody to determine the surface expression or were incubated with increasing molar concentrations of recombinant GluA4-Fc protein before staining with a huIgG1-Fc specific antibody (rows 2-10).

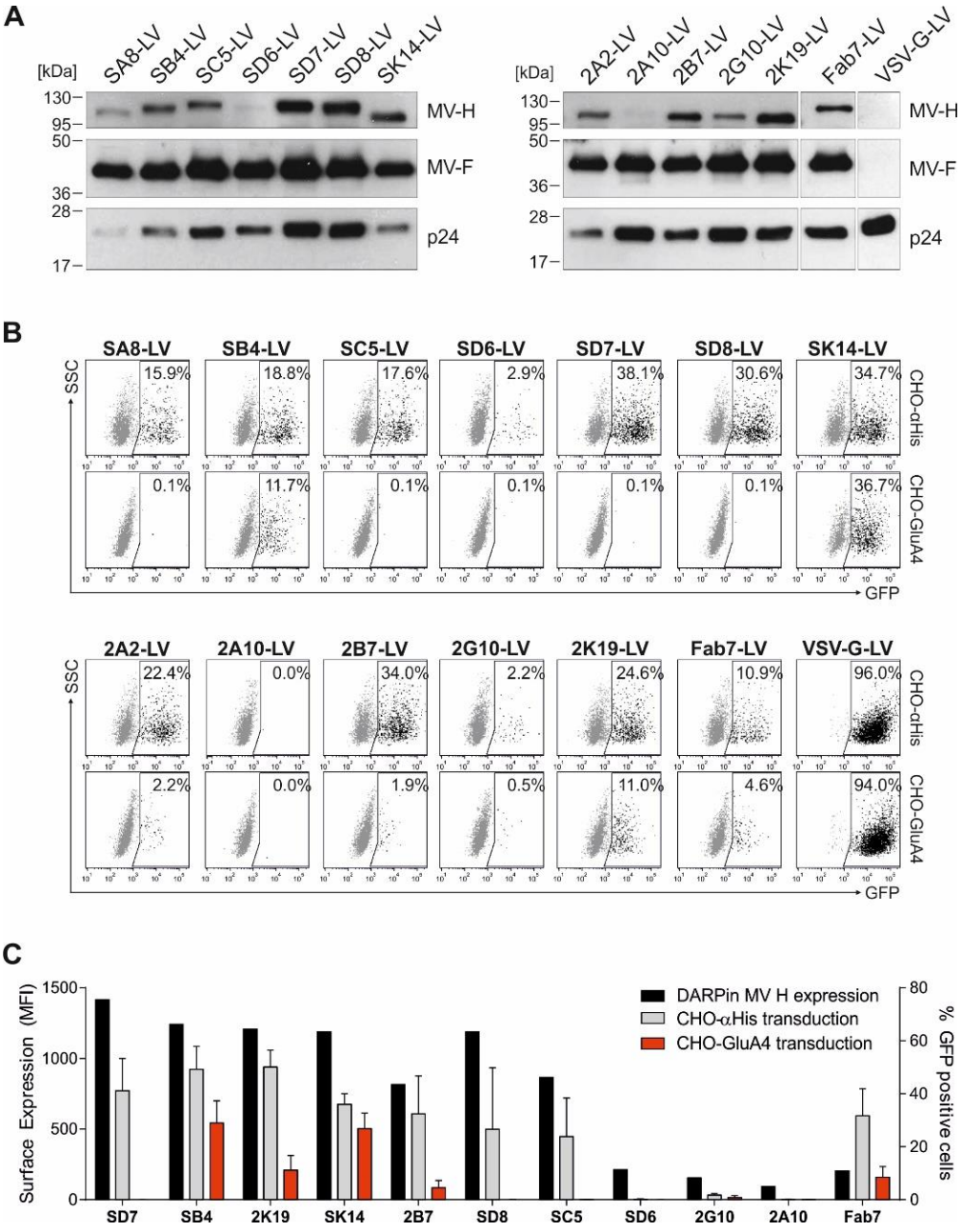

Figure S9: Comparision of H-DARPin and F incorporation into LV vectors and vector transduction efficacy.

(A) Western Blot analysis of the indicated LVs. Particle amounts corresponding to 5 µl concentrated vector stock were loaded onto a 10% SDS gel. Proteins were detected utilizing anti-MV-F, anti-MV-H, or anti-p24 antibodies. LV particles displaying the scFv Fab7 instead of a DARPin or pseudotyped VSV-G were used as controls. **(B)** Transduction of CHO-αHis or CHO-GluA4 cells with 1 µl of indicated concentrated vector stocks used for western blot analysis in (A). Cells were analyzed for GFP expression 72 h post transduction by flow cytometry. The percentage of GFP positive cells is indicated. **(C)** Bar diagram of DARPin-H cell surface expression and transduction of CHO-αHis or CHO-GluA4 cells of indicated DARPins and the scFv Fab7 from Figure 7. Left scale: median fluorescent intensities (MFI) of surface stained DARPin-H or Fab7-H proteins after transient transfection of HEK293T cells with the corresponding expression plasmids. Right scale: percentage of GFP-positive CHO-αHis or CHO-GluA4 cells transduced with LV particles displaying the indicated DARPins or Fab7. Each transduction experiment was performed at least three times with individually small scale produced vector particles, showing mean values and standard deviations.

Supplementary Tables

Table S1: Calculated diversity of the assembled DARPin libraries and intermediates.

Fragment[1]	Size	Amount of DNA[2]	Diversity[3]
Ncap-DAR (N1)	228 bp	910 ng	$3.89x10^{12}$
Ncap-DAR-DAR (N2)	327 bp	5835 ng	$1.74x10^{13}$
Ncap-DAR-DAR-DAR (N3)	426 bp	8364 ng	$1.90x10^{13}$
Ncap-DAR-DAR-Ccap (N2C)	393 bp	5736 ng	$1.42x10^{13}$
Ncap-DAR-DAR-DAR-Ccap (N3C)	492 bp	9240 ng	$1.83x10^{13}$
T7-N2C-Spacer	1300 bp	40.8 µg	$3.06x10^{13}$
T7-N3C-Spacer	1399 bp	53.8 µg	$3.75x10^{13}$

[1] For product nomenclature refer to Fig. S1

[2] Recovered ligation products after gel extraction

[3] Calculated theoretical diversity based on the fragment size and amount of recovered DNA.

Table S2: Primer sequences for plasmid construction.

Primer	No.	Sequence (5' to 3')
huFc for	1	CTAGCTAGCGACAAAACTCACACATGCCCACCGTGCCCAGCACCTGAAC
huFc-G4S-Avi rev	2	CGAGGCTGATCAGCGAGCTTCTAGATATTATTCATGCCACTCAATCTTCTGAGCTTCGA AAATGTCGTTAAGGCCGGAGCCCCCTCCGCCTTTACCCGGGGACAGGGAG
BirA for	3	TATCAGGGCCCAGCCGGCCAGATCTATGAAGGATAACACCGTGCCACTG
BirA-ER rev	4	CCGCTCGAGCGGCCGCGTCGACTCACAGCTCGTCCTTTGAACCCCCAGATCCAGATGT AGA CCCTTTTTCTGCACTACGCAGGGATATTTC
BirA rev	5	GAGGCTGATCTCGAGCGGCCGCGTCGACTCATTTTTCTGCACTACGCAGGGATATTTC
HA-Oligo for	6	AATTCATTAAAGAGGAGAAATTAACTATGAGAGGATCGCATCACCATCACCATCACGG TTCTTATCCATATGATGTTCCAGATTATGCTGCGGCCCAGC
HA-Oligo rev	7	GGGCCGCAGCATAATCTGGAACATCATATGGATAAGAACCGTGATGGTGATGGTGAT GCGATCCTCTCATAGTTAATTTCTCCTCTTTAATG
3xSTOP Oligo for	8	CGGCCCAGGTCCAGCTGCAGGAATCCGGGCCCAGATCTGCCGGCCGCGGCCGCTTAA TTGATTGACACGCAGTGTGATTGATTGAGCCAGTGGCGTGGTTAAT
3xSTOP Oligo rev	9	TAACCACGCCACTGGCTCAATCAATCACACTGCGTGTCAATCAATTAAGCGGCCGCGG CCGGCAGATCTGGGCCCGGATTCCTGCAGCTGGACCTGGGCCGGCT
CD015-DARPin for	10	AAATTTGGCCCAGCCGGCCGACCTGGGTAAGAAACTGCTGGAAG
CD105-DARPin rev	11	TGTACAGAGCGGCCGCATTAAGCTTTTGCAGGATTT

Table S3: DNA sequence of codon optimized DNA fragments used for DARPin library assembly.

Fragment	Sequence (5' to 3')[1]
Ncap	GGCCCAGCCGGCC**GACCTGGGTAAAAAACTGCTGGAAGCAGCACGTGCAGGTCAGGATGATGAAGT TCGTATTCTGATGGCAAATGGTGCAGAC**GTGAGACCTTAGGAATTC
Ccap	GCTAGCTAGGAAGACCT**GACGTTAATGCCCAGGATAAATTTGGTAAAACACCGTTTGATCTGGCCA TTGATAATGGCAATGAAGATATTGCCGAAGTGCTGCAGAAAGCAGCA**GCGGCCGCTCACGCAGTGG AATTC
AR	GGATCCTAGGAAGACCT**GACGTTAACGCA*NNN*GAT*NNNNNN*GGT*NNN*ACACCGCTGCATCTGGCAG CA*NNNNNN*GGTCATCTGGAAATTGTTGAAGTGCTGCTGAAA*NNN*GGTGCAGACGTG**AGACCTTAGA AGCTT

[1]Coding regions are depicted in bold.

Table S4: Primer sequences for DARPin library generation.

Primer	**No.**	**Sequence (5’ to 3’)**
Ncap for	1	CGCGGATCCGACCTGGGTAAAAAAC
AR rev	2	AGATCTAGGCCTTCTAGACCCAAGC
Lib for	3	AAATTTGGCCCAGCCGGCCGACCTGGGTAAAAAAC
Lib rev	4	CCGGAATTCCACTGCGTGAGCGGCCGCTGCTGCTTTCTGCAGCACTTCGGCAATATC
T7 for	5	AGGGAGAAAGGCGGACAGGTATCCGGTAAGCG
T7 rev	6	AACTATCAGGGCCGGCTGGGCCGCGTGATG
Spacer for	7	ATAAGAATGCGGCCGCTCACGCAGTGGAATTCGGATCTGGTGGCCAGAAG
Spacer rev	8	AAAGGGAATAAGGGCGACACGG
T7B	9	ATACGAAATTAATACGACTCACTATAGGGAGACCACAACGG
TolAk	10	CCGCACACCAGTAAGGTGTGCGGTTTCAGTTGCCGCTTTCTTTCT

Supplementary Methods

DARPin detection in crude cell extract and binding assay by ELISA – Detection of DARPins within crude *E. coli* extracts and DARPin binding analysis was performed on the basis of previously described protocols[1,2]. In brief for detection of DARPins within crude *E. coli* extracts, 96-well Maxisorb plates (Nunc) were coated with 1 µl of crude DARPin containing *E. coli* extracts in a total volume of 100 µl TBS overnight at 4°C. After washing the wells three times with 300 µl TBS-T (TBS, 0.1% Tween-20), unspecific binding was blocked by addition of 300 µl TBS-TB (TBS, 0.1% Tween-20, 0.5% BSA) per well for 1 h at room temperature. Subsequently, wells were incubated with a biotin-conjugated mouse anti-PentaHis antibody (1:2000; Qiagen, 34440) and HRP-conjugated streptavidin (1:500; Jackson ImmunoResearch, 016-030-084) for 1 h at room temperature. The plates were washed three times with TBS-T after each antibody incubation step. The bound antibodies were detected using SureBlue TBM substrate (KPL) and 1 N H_2SO_4. The reaction product was quantified in a microtiter plate reader at 450 nm.

To determine target binding of DARPins within crude *E. coli extracts,* 96-well Maxisorb plates (Nunc) were coated with 20 µM neutravidin diluted in TBS for 1 h at room temperature. After washing the wells three times with 300 µl TBS-T, unspecific binding was blocked by addition of 300 µl TBS-TB per well for 1 h at room temperature. Next, wells were incubated with 20 nM recombinant target protein diluted in TBS-TB overnight at 4°C. After washing the wells three times with 300 µl TBS-T, each well was incubated with 2.5 µl of crude DARPin containing *E. coli* extracts in a total volume of 100 µl TBS for 1 h at 4°C. Wells were washed three times with 300 µl TBS-T before subsequent incubation with a mouse anti-RGSHis antibody (1:2000; Qiagen, 34650) and a HRP conjugated rabbit anti-mouse antibody (1:2000; DAKO, P0260) for 1 h at room temperature. The plates were washed three times with TBS-T after each antibody incubation step. The bound antibodies were detected using SureBlue TMB substrate (KPL) and 1 N H_2SO_4. The reaction product was quantified in a microtiter plate reader at 450 nm.

Surface Expression – Flow cytometry analysis was performed on the MACSQuant Analyzer 10 (Miltenyi Biotec, Bergisch Gladbach, Germany). Surface expression of GluA1-4 and GluR6 on the respective CHO cell line was detected by staining with PE-coupled myc antibody (clone 9B11; 1:100; Cell Signaling Technology) in case of CHO-GluA4, or PE-coupled FLAG antibody (clone M2; 1:100; Abcam) for all other investigated cell lines. As control, cells were incubated without antibody.

LV particle production for SDS-PAGE – Lentiviral vector were generated by transient transfection using PEI as described previously with some minor modifications as indicated. In brief, 24 h prior to transfection, $9x10^6$ HEK-293T cells were seeded in one T75 flask. On the day of transfection, the cell culture medium was replaced by 10 ml DMEM+FCS. For the transfection mix, 15 µg of total DNA was mixed with 990 µl of DMEM without additives and added to 930 µl DMEM supplemented with 60 µl of 18 mM PEI solution per T75 flask. After incubation for 20 minutes at room temperature, the transfection mix was added to the HEK-293T cells. 24 h later, the medium was replaced by 10 ml fresh cell culture medium. At day two post transfection, the cell supernatant was filtered (0.45 µm filter) and concentrated and purified by centrifugation at 4,500x g over a 20% sucrose cushion for at least 24 hours at 4°C. The pellet was resuspended in 50 µl PBS. For LV-targeting vectors, 580 ng of DARPin-H or scFv-H plasmid, 1.73 µg of MV-F plasmid, 6.2 µg of the packaging plasmid pCMVΔR8.9 and 6.5 µg pSEW were used for transfection. LV particles pseudotyped with VSV-G were produced by co-transfection of 2.6 µg pMD.G2 along with 4.9 µg pCMVΔR8.9 and 7.5 µg pSEW.

Supplementary References

1. Dreier, B. and Plückthun, A. (2012). Rapid selection of high-affinity binders using ribosome display. Methods Mol. Biol. 805, 261–286.
2. Steiner, D., Forrer, P. and Plückthun, A. (2008). Efficient selection of DARPins with sub-nanomolar affinities using SRP phage display. J. Mol. Biol. 382, 1211–1227.